1-1-1968

Kinetic study of the catalytic oxidation of carbon monoxide.

Vinod C. Khera
University of Windsor

KINETIC STUDY OF THE CATALYTIC OXIDATION OF CARBON MONOXIDE

A Thesis
Submitted to the Faculty of Graduate Studies through the Department of Chemical Engineering in Partial Fulfilment of the Requirements for the Degree of Master of Applied Science at the University of Windsor

by

Vinod C. Khera

Windsor, Ontario
1968

A13F 4319

APPROVED BY: Alex Grusso

G. P. Mathur

Robert C. Rumsfeldt

209980

ABSTRACT

A catalytic reactor was designed and constructed to study the kinetics of a highly exothermic reaction, namely the oxidation of carbon monoxide, under integral plug flow conditions. The reactor was found to be an efficient unit that could be used under isothermal conditions with a commercial 0.3 % Pd on alumina catalyst in the form of 1/8" X 1/8" pellets.

Data were taken at the temperatures of 170°, 180°, and 195°C; and at pressures close to atmospheric. The range of conversion was from 20 % to 60 %. Mass and heat transfer effects on kinetics were found to be negligible.

The rate model which was found to fit the data most satisfactorily is as follows:

$$(-r_{CO}) = 7.4 \exp(-27{,}900/RT)\frac{(O_2)}{(CO)}$$

This rate equation signifies either the surface reaction between chemisorbed carbon monoxide and oxygen or the chemisorption of oxygen as the rate controlling step. The data were found to fit the rate equation within 95 % confidence limits for all the temperature levels investigated.

ACKNOWLEDGEMENTS

The author wishes to take this opportunity to express his deep admiration and gratitude to Dr. Guru P. Mathur for his interest and able guidance, valuable criticism and encouragement throughout the course of this investigation. Dr. Maurice Adelman and Dr. Alex Gnyp also provided useful suggestions.

The author is also thankful to Mr. Louis F. Cory of the Electronics shop for assistance in the maintenance of the Gas Chromatograph and to Mr. Halil Parlar for assisting in the build up of the experimental set-up.

The financial support for this work was provided by the National Research Council of Canada.

CONTENTS

FIGURES

TABLES

I. INTRODUCTION

The harmful effects of air pollution are felt not only in a city like Los Angeles, but also in the smaller ones. Automotive exhaust is by far the most significant air pollutant in the cities. The exhaust gases from the internal combustion engines are complex mixtures consisting principally of the products of hydrocarbon combustion, and small amounts of the oxidation products of sulphur and nitrogen. The major constituents are water, CO_2, N_2, O_2, CO, and H_2; whereas minor constituents are oxides of sulphur and nitrogen, aldehydes, organic acids, alcohols, hydrocarbons, smoke etc. (11). Table I.1 in Appendix I gives a typical composition of exhaust gases.

Carbon monoxide constitutes the largest single component contributing to air pollution from automotive exhausts. Carbon monoxide gas is extremely toxic and because of this, it is extremely dangerous in enclosed spaces where it may even cause death. It has also been found to be an asphyxinal which combines with the hemoglobin of blood (19). Tables I.2 and I.3 in Appendix I list the effects of carbon monoxide concentrations on the human body.

The emmission standards for exhaust gases as set by the U.S. State Department of Health are not over 1.5 %

by volume of carbon monoxide and 375 p.p.m. hydrocarbons which reflect approximately an 80 % reduction of hydrocarbons emissions and a 60 % reduction of carbon monoxide (12).

The automobile industry and many research organizations have been concerned with minimizing the quantity of air pollutant components from automotive exhausts. The work of these people has been hampered by the lack of high temperature materials of construction and development of catalysts which would be immune to poisoning. The industry has also been concerned with evaluating various methods of reducing air pollution from automotive exhausts including modifications of the design of the engines etc. A number of operational and performance penalties have, however, been experienced (3). It appears that in order to bring down the quantity of carbon monoxide and hydrocarbons to an acceptable level, their oxidation will eventually be necessary.

The problem of catalyst poisoning is an important one still to be solved. It is hoped that a system can be developed which would remove various catalyst poisons from the exhaust gases before they are allowed to come in contact with the catalyst or a catalyst would be prepared which will not be poisoned by the lead oxide and water vapour present in the exhaust gases.

Conventional integral plug flow reactors have been found to be rather unsuitable for highly exothermic reactions like carbon monoxide oxidation because of the

problems involved in maintaining isothermal conditions in such a system as mentioned by Tajbl et. el. (24).

The temperature control problems associated with such a system and the presence of carbon monoxide as a major constituent in automotive exhausts suggested a careful and systematic investigation of the catalytic oxidation of carbon monoxide.

The feasibility of using the conventional plug flow type of integral reactors for kinetic study by means of slightly modified design and deviation from the usual operating procedure is studied in this investigation. The reactor was not heated directly, whereas preheating of the reactant gases was utilized directly and the heat of reaction was utilized indirectly in order to control the temperature of the integral reactor during the course of this investigation.

The purpose of the present investigation is two-fold:

1. To study the feasibility of using an integral plug flow catalytic reactor for a significant level of conversions for the highly exothermic reactions. The reaction chosen was the catalytic oxidation of carbon monoxide with air over 0.3 % palladium catalyst supported on alumina.
2. To study the kinetics of the above mentioned reaction and to establish the rate equation and determine the reaction velocity constants of the temperature range of 170° to 195°C and also to determine the energy of activation.

The rate equation established in this study may be used in the design of a suitable catalytic reactor.

II. LITERATURE SURVEY

An extensive survey on the catalytic oxidation of carbon monoxide has been prepared by Katz (16). Dixon and Longfield (10) have also reviewed the literature on carbon monoxide oxidation on Ag, Pd and oxide catalysts.

Carbon monoxide oxidation occurs readily at high temperatures as low as room temperature by transition metal oxide catalysts such as MnO_2, CuO, NiO and CoO. Multicomponent catalysts with mixtures of oxides of Mn, Cu, Co and Ag are particularly active in the oxidation of carbon monoxide and are known as Hopcolites. Detailed information on important catalysts can be found elsewhere (1, 2, 13, 20, 23). The most commonly employed catalysts are weakly basic oxides of the transition metals (e.g., oxides of Zn, Cu, Pb, Ti, Mn, Fe, Ni, Co and Mo), Pt and Pd in their metallic state, the oxides of Ag and Hg and the weakly acidic oxides of Cr, Mn, Fe, and Mo and oxides of rare earths (e.g., cerium and thorium).

In the case of chemisorption of carbon monoxide on oxide catalysts, it has been observed (16) that some gas is at first adsorbed instantaneously followed by a slow adsorption which varies approximately as the square

root of time and is not appreciably dependant upon the pressure. It is interesting to note here that the mobility or the translational freedom of the adsorbed molecules can be determined from a knowledge of the entropy of adsorption. This has been illustrated by Damkohler and Edse (8).

A recent review by Dixon and Longfield (9) cites the work of Schwab and Grossner (21) in which the rate of carbon monoxide oxidation over palladium wire was described by the relationship:

$$-\frac{d(CO)}{dt} = k\frac{(O_2)}{(CO)} \qquad \ldots(2.1)$$

which is a simplified form of the expression where oxygen chemisorption is the rate controlling step, i.e.,

$$-\frac{d(CO)}{dt} = k\frac{(O_2)}{1 + K(CO)} \qquad \ldots(2.2)$$

When carbon monoxide adsorption on Pd wire is high , Eqn. 2.2 reduces to Eqn. 2.1. In general, however, Schwab's work suggests an expression of the form:

$$-\frac{d(CO)}{dt} = k\frac{(O_2)(CO)}{(1 + K(CO))^2} \qquad \ldots(2.3)$$

in which the surface reaction between carbon monoxide and oxygen is the rate controlling step. In the case of high adsorption of carbon monoxide gas on palladium, when $K(CO) \gg 1$, Eqn. 2.3 redues to Eqn. 2.1. Modell's work (18)

on Pd wire also agrees with the work of Schwab, whereas the results of Daglish and Eley (7) are in direct conflict with those of the above investigators. They suggested dissociative chemisorption of oxygen as the rate controlling step. The work of Daglish and Eley was carried out at lower temperatures as compared to others; which could probably explain the shift in mechanism. For high adsorption of CO on Pd, this can be written as follows:

$$(-r_{CO}) = k \frac{(O_2)}{(CO)^2} \qquad \ldots(2.4)$$

The works mentioned above have been on Pd wire and films as catalyst surfaces. The only work on the kinetic investigation of CO oxidation on a Pd catalyst supported on alumina is that of Tajbl et. al. (24). Their study was carried out on in a continuous stirred tank catalytic reactor for conversions upto 15 %. This reactor was considered superior to the conventional plug flow reactor mainly because the plug flow reactors are extremely difficult to operate under isothermal conditions. The rate model suggested was first order with respect to O_2 concentration and inversely proportional to the CO concentration.

The investigations mentioned above are based on the assumption that carbon monoxide is very strongly adsorbed on Pd. This has been confirmed in the work of Stephens(22) who studied the adsorption of the carbon monoxide-oxygen system on palladium metal film. It was however not possible in his work to establish oxygen adsorption rates in the

presence of carbon monoxide as they encountered the expected diffculties of reaction between adsorbed carbon monoxide and oxygen, wheras there is no use of finding the oxygen adsorption rates in the absence of carbon monoxide because the palladium surface changes its adsorptive characteristics by the presence or absence of carbon monoxide.

The complete rate equations for the various rate controlling steps, the simplified forms of which have been mentioned in this chapter will be discussed in detail in Capter III.

III. THEORY

A. Catalytic Kinetics

The determination of the kinetics of a chemical reaction, in general, and a catalytic reaction, in particular, involves the understanding of the fundamentals of the process. Unfortunately, very little is known about the exact role of a catalyst in a catalytic reaction. So far, insufficient knowledge exists on the total phenomenon. Under the present circumstances until a more comprehensive understanding of the catalytic phenomenon is achieved, there are two approaches open to the present day investigator. One is based on the Langmuir-Hinshelwood mechanisms as modified and propounded by Hougen and Watson; and the other approach is through the empirical power law formulation.

Hougen and Watson (15) proposed the following steps by which a catalytic reaction proceeds:

1. Mass diffusion of the reactants to the exterior surface of the catalyst.

2. Diffusion of the reactants into the catalyst pore structure.

3. Chemisorption of the reactants on the active sites of the catalyst.

4. Surface reaction between chemisorbed reactants

and/or reactants in the gas phase.

5. Desorption of products.

6. Diffusion of the products out of the pores to the exterior surface.

7. Mass diffusion of the products away from the surface of the catalyst.

Steps 1, 2, 6, and 7 are physical in nature whereas the rest of the steps are chemical ones.

One or more of the seven steps could be rate controlling. The rate expressions for single rate controlling steps have been proposed by Yang and Hougen (26). In those cases where two surface reactions are occuring simultaneously on different types of active sites, the two reaction rates are additive requiring independant rate equations.

B. Evaluation of Rate Equations

When the diameter of the catalyst particles is small in comparison with the tube radius, a flat velocity profile is obtained and this acts as a condition confirming plug flow behaviour in the reactor (25). For the case when a steady state flow system exists, if an elemental section of the reactor is considered with a catalyst mass of dW producing a conversion of dX of the reactant, then the basic conversion equation can be written as:

$$F\ dX = (-r_A)\ dW \qquad \ldots(3.1)$$

where F = lb. moles/hr. of feed.

X_A = conversion in lb. moles of A/lb. mole of feed.

$-r_A$ = molal rate of disappearance of reactant A based on unit mass of the catalyst.

W = mass of the catalyst, lbs.

This equation can be rewritten in the integrated form as:

$$\frac{W}{F} = \int_0^{X_A} \frac{dX_A}{(-r_A)} \qquad \ldots(3.2)$$

The expression for the reaction rate is substituted in Eqn. 3.2 in terms of conversions taking into account any expansion or contraction in volume of the feed stream during the course of the reaction. The right hand side of Eqn. 3.2 is then integrated and the integrated expression plotted as abscissa against W/F as ordinate. In case the integrated right hand side is a complicated expression, then multi-linear regression can be employed and the values of the constants in the rate expression evaluated.

For rate expressions which are highly complicated, the integration is best carried out graphically although this method is rather inaccurate.

Since an integral reactor was employed in this study, instantaneous numerical values of reaction rates at various conversions can be computed by differentiating the X vs. W/F curve. This however introduces graphical differentiation errors and is therefore not generally used.

C. Effectiveness Factor

The effectiveness factor E, is defined as the ratio of average reaction rate within a pore to the maximum reaction rate if the pore is absent, i.e., if all the interior surface is equally available at the temperature, pressure and composition prevailing at the exterior surface. An effectiveness facor of unity is approached when the size of the catalyst particles is small, and when the pores are large and well interconnected (19). With the small sized and highly porous catalyst used in this study, these conditions are conveniently met. Therefore an effectiveness factor of unity was assumed.

D. Axial Aspect Ratio

Axial aspect ratio has been defined as the ratio of the length of the catalyst bed to the catalyst particle diameter (Z/d_p). According to Carberry (5), axial mixing effects upon kinetics can be ignored safely and plug flow kinetic behaviour for all kinetic orders will be insured if axial aspect ratios of at least 30 are used in integral plug flow reactors.

A sufficiently large axial aspect ratio should, therefore be used (an axial aspect ratio of 60 was chosen based upon the quantity of the catalyst required for significant conversions) so that the axial mixing does not affect the kinetic study.

IV. EXPERIMENTAL EQUIPMENT

The design and construction of the experimental equipment constitutes an essential part of this project. The detailed diagram of the catalytic reactor is shown in Fig. 1, whereas a schematic diagram of the experimental set-up is shown in Fig. 2.

A. Major Equipment

1. Reactor

A cylinderical tubular reactor was used in this experimental investigation. The reactor was made from a 2 foot long 1-1/2 in. 16 BWG mild steel tube surrounded by a concentric 2 in. sch. 40 mild steel pipe. The annulus was provided in order to (i) utilize the heat of effluent gases from the reactor in heating the reactor, (ii) to act as an insulation on the reactor tube because of the very low thermal conductivity of the gases. Standard 150 lb. mild steel flanges for 2 in. sch. 40 steel pipe were welded at the two ends of the reactor. The flange at each end was fitted with one screwed 1/4 in. Swagelok 316 stainless steel male connector for flexibility in connection to inlet and outlet tubing and to facilitate insertion of Berl Saddles. One screwed Omega connection was also provided on each flange for flexibility in the adjustment of thermocouple

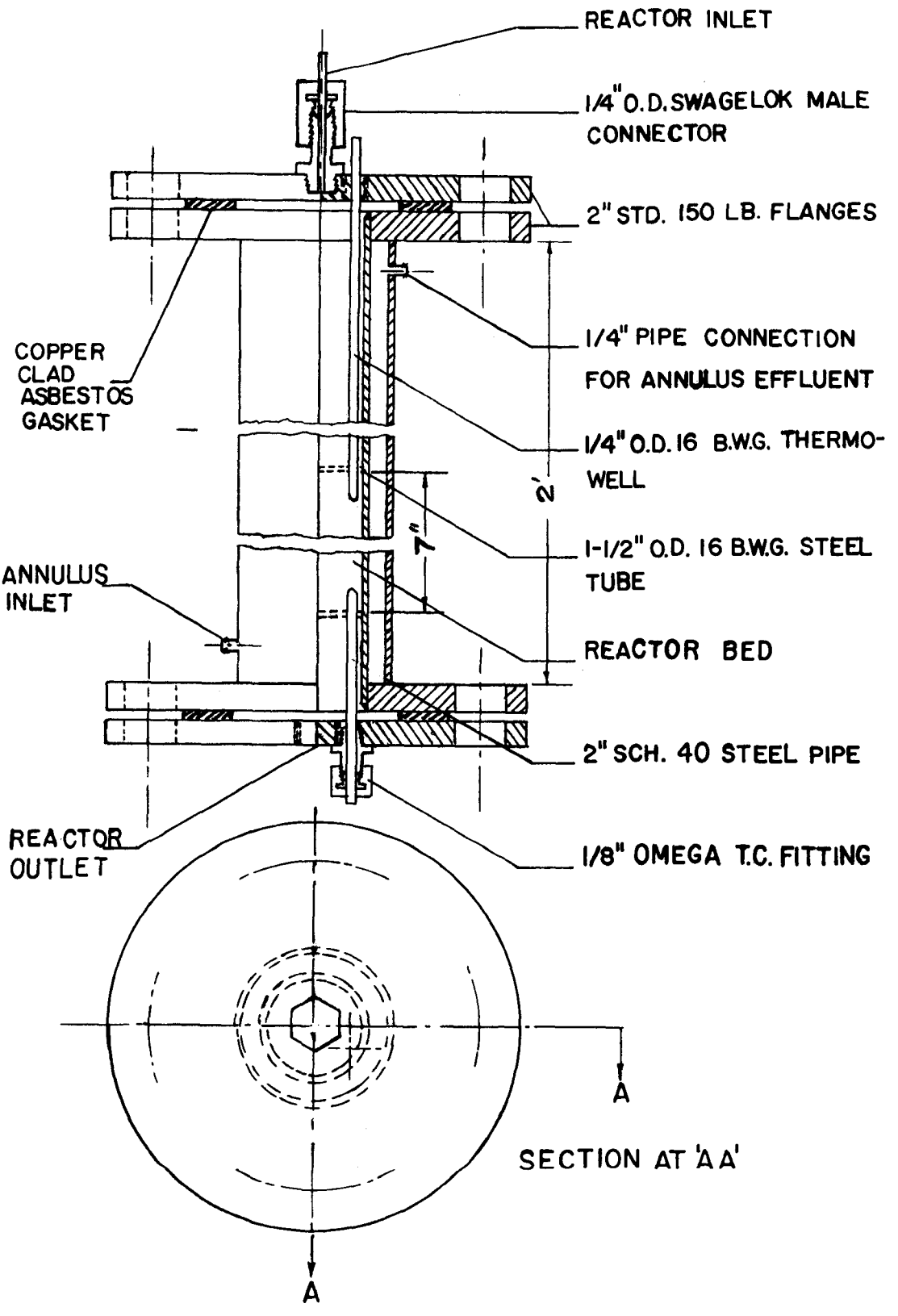

FIG. 1 SECTIONAL VIEW OF THE REACTOR

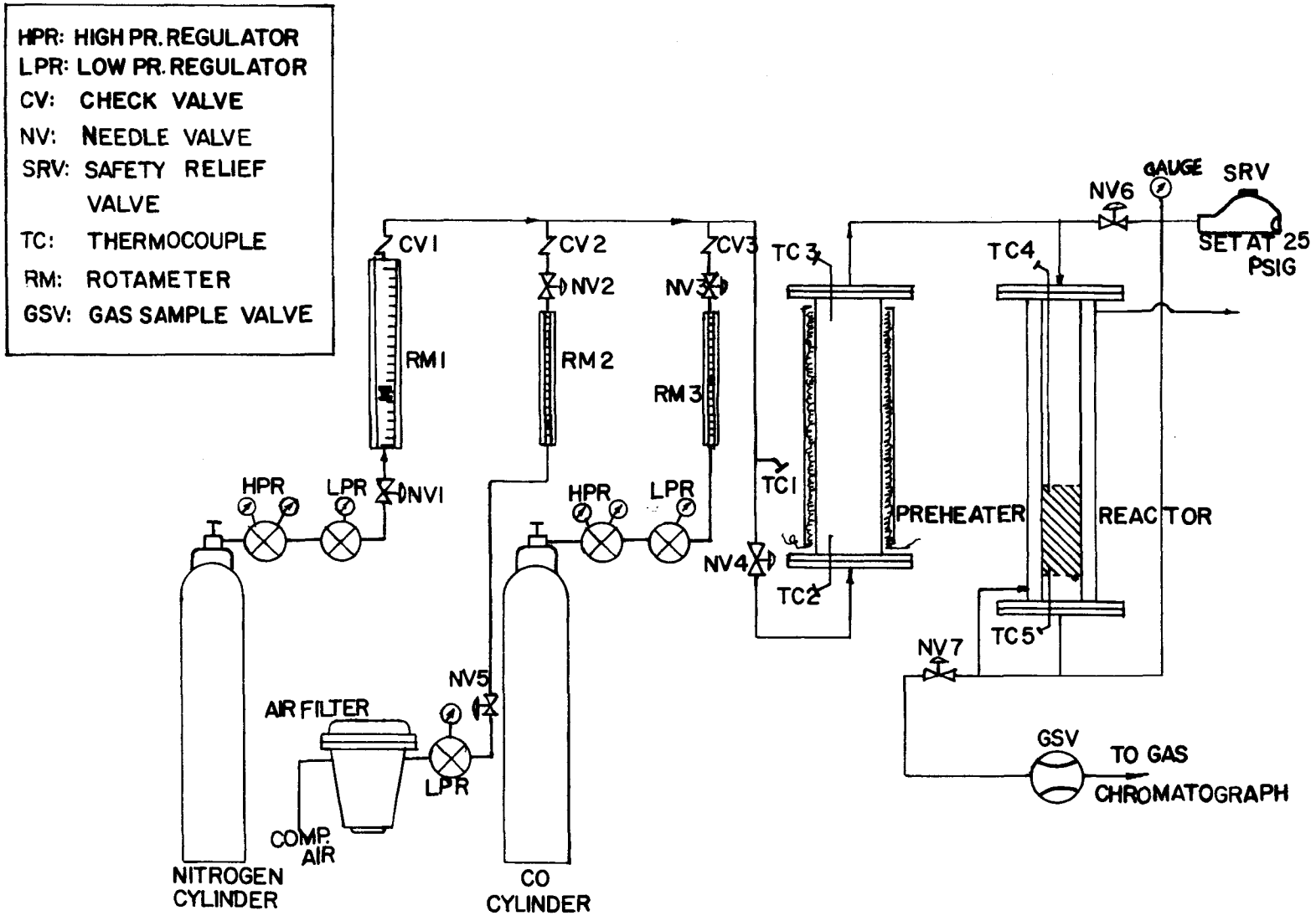

FIG. 2 SCHEMATIC DIAGRAM OF EXPERIMENTAL SET UP

protection tubes.

The outlet for the reactor effluent gases was connected to the inlet of the annulus located at the lower end of the reactor so that these gases pass through the annulus leaving it at the outlet which is located at its upper end.

The catalyst bed was held by means of two 1/16 in. thick stainless steel screens snugly fitting inside the reactor tube. The empty space below the catalyst bed was filled with ceramic berl saddles to act as a support to the catalyst bed. The catalyst bed was filled with the catalyst mixed with the berl saddles. The details of the catalyst used in this investigation are given in Table I.6 in Appendix I.

2. Preheater

The preheater consisted of a 2 in. sch. 40 mild steel pipe with standard 150 lb. steel flanges welded at both ends. The fittings on each of the top and bottom flanges are identical to those on the reactor flanges.

The heat to the preheater was supplied by two 18 in. long, model 50241 type 2718-SP semi-cylinderical heating units each rated at a maximum wattage of 940.

B. Process Measurements and Control

1. Flow Measurement and Control

Rotameters were used for all flow measurements. The nitrogen gas rotameter was fitted with 1/2 in. o.d., 16 BWG copper tube which was used with all the rotameters except the N_2 gas rotameter. For the latter, a ½ in. to ¼ in.

Swagelok reducer was used downstream from the rotameter before mixing of the nitrogen gas with the rest of the gases took place.

Brass check valves with neoprene o- rings and stainless steel screens were used at the outlet of each rotameter to prevent backmixing of the gases.

2. Temperature Measurement and Control

The temperatures of the gases entering and leaving the preheater were measured by 1/16 in. od. 20 gauge series 1000 chromel alumel thermocouples supplied by Thermocouple Products Co. The thermocouples were enclosed in 1/8 in. o.d. stainless steel protection tubes which were positioned in the flanges by means of 1/8 in. Omega stainless steel thermocouple connectors. Some static electricity was observed to develop. Grounded thermocouples gave an error of the order of 2 to 3 mV. Since accurate temperature measurement for the preheater inlet was not necessary, a rough measurement was accepted for the preheater inlet gases. In the case of the preheater outlet and reactor bed temperatures, ungrounded thermocouples were used. This type of thermocouples was not affected by the static electricity developed in the equipment. The thermocouples in the catalyst bed were kept at a distance of one inch from the two ends of the bed, while providing for the necessary flexibility of movement of the thermocouples for checking temperature variation inside the

catalyst bed.

A selector switch was used for thermocouple connections. The positive terminals of all the thermocouples were combined whereas the negative terminals were individually connected to various points on the selector switch. The leads from the selector switch were connected to a potentiometer through an ice junction.

The temperature of the gases leaving the preheater was controlled by adjusting the voltage of a 20 ampere model 9-521-10V2 variable transformer supplied by Fischer Scientific Co. This transformer controlled the heating from the semi-cylinderical heaters surrounding the preheater.

The heat loss from the gas lines from preheater outlet to reactor inlet and from reactor outlet to annulus inlet were controlled by controlling the voltage supply to heating cords by means of two 10 amperes model 9-521-5V2 variable transformers supplied by Fischer Scientific Co.

The temperature of the catalyst bed was controlled in two ways:

a. By controlling the temperature of the gases entering the reactor.

b. By controlling the recirculation of hot gases in the annulus.

3. Pressure Measurement and Control

The pressures of carbon monoxide and nitrogen gases which were taken from gas cylinders were controlled by model 1L pressure regulator coupled to model 70A low press-

ure regulator supplied by the Matheson Company.

The pressure for each gas was measured at rotameter inlet conditions using pressure gauges of the following ranges:

Nitrogen gas	0 to 100 psig
Rest of the gases	0 to 10 psig

Higher range of pressure was used for nitrogen gas because of its high flow rates. The pressure at the inlet and outlet of reactor was measured by a pressure gauge of range 0 to 10 psig by using two control valves.

A safety relief valve set at 25 psig was installed after the reactor pressure gauge as shown in Fig. 2.

C. Analytical Equipment

The reactant and product gases were analysed using a series 5,000 selecta system gas chromatograph supplied by Barber-Colman Co. of Canada Ltd. This included an injector bath, a column bath followed by a detector bath, a six port thermal conductivity detector with W2-X filaments and power supply module to the filaments. The arrangement of the thermal conductivity detector is shown in Fig. 3. The signals from the detector were recorded on a strip chart recorder. The temperature of the individual units was controlled by the control arrangements provided on the gas chromatograph.

The injected sample gases passed through a silica gel column in a 1/4 in. o.d., 1 ft. long copper tubing followed by a second column of molecular sieves, which was 11 ft.

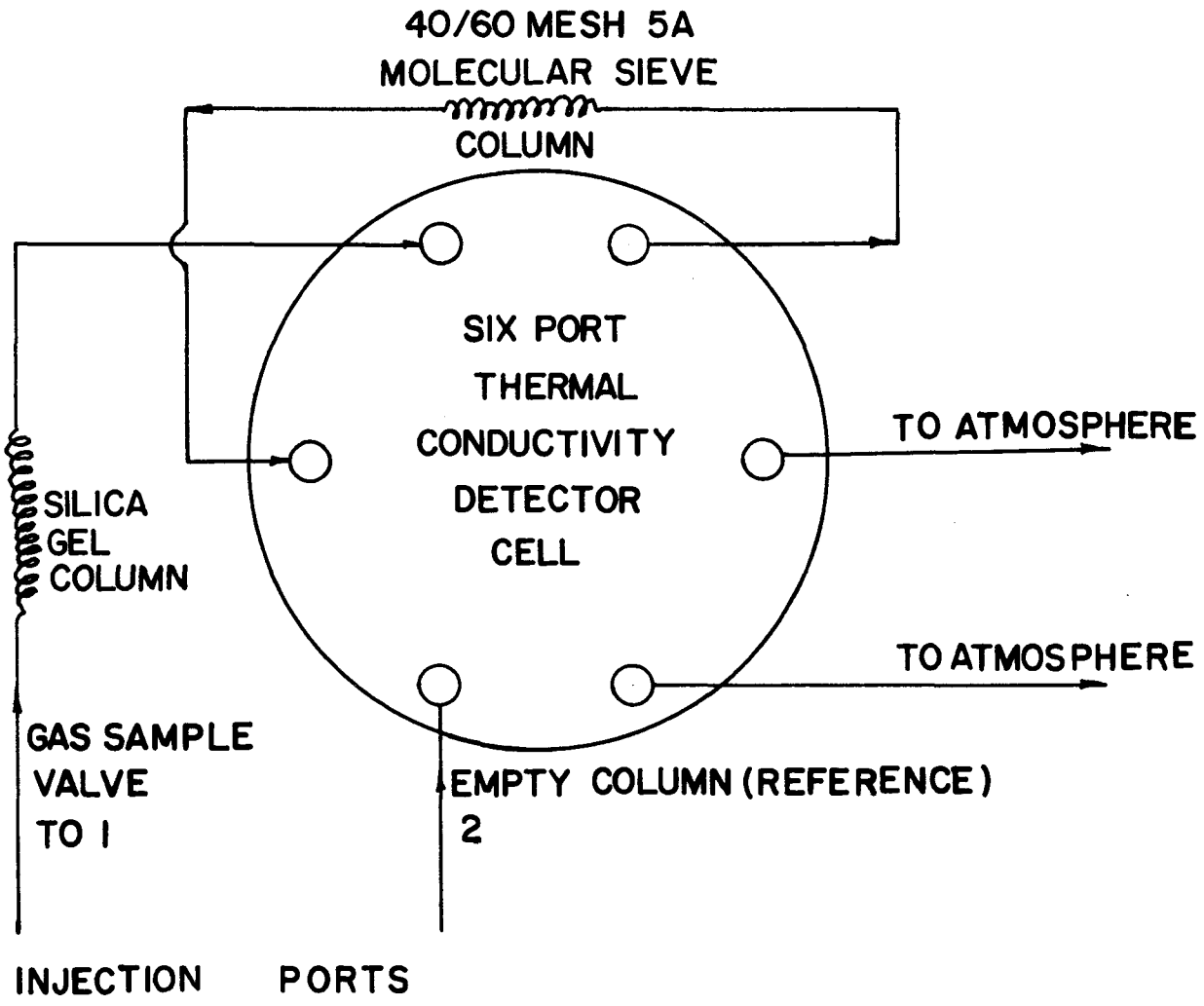

FIG. 3 ARRANGEMENT OF THERMAL CONDUCTIVITY DETECTOR

long in a 1/4 in. o,d. copper tubing. The molecular sieve was 5 A, mesh size 40/60 supplied by the Chromatographic Specialities Ltd. The second column acted as a reference column and was a 1/8 in o.d. empty copper tubing. Standard 0.13 ml gas sampling valve supplied by Barber-Colman Co. of Canada Ltd. was used as Hamilton Gas Tight syringes were found to be completely unsatisfactory for the precision required.

The silica gel column gave separation of carbon dioxide gas from the rest of the gases, whereas the molecular sieves column gave explicit separation of oxygen, nitrogen, and carbon monoxide in their order of appearance. The bands of various gases were fairly well resolved because the lengths of the columns were decided after some trial and error. The optimum column lengths were used to get the best possible separation and a distinct distribution of residence times of the gases in the columns.

Carbon dioxide was irreversibly adsorbed on the molecular sieves, however, since the quantities of carbon dioxide injected is very small as compared to the amount of molecular sieves, the latter was very slowly destroyed.

V. EXPERIMENTAL PROCEDURE

The experimental procedures consisted of the following:

A. Calibration of Rotameters

All the rotameters were calibrated using a Wet Test Gas Meter supplied by Precision Scientific Co. Inlet temperature and pressure conditions were used for this calibration. All the rotameter needle control valves were kept at the outlet as suggested by the manufacturer. The volumetric flow rates at the conditions of calibration were then converted to standard conditions (14.7 psia, 70°F) and molar flow rates were calculated. These were then plotted vs. rotameter scale reading (error was ± 2%.).

B. Operation of Gas Chromatograph

The following sequential operation was carried out:

1. The flow rate of helium through each of the two columns was adjusted to 40 ml./min. within ± 5 % of each other.

2. The detector heat was switched on and temperature controlled at the desired level of 100°C by means of adjustment on the detector heat control module.

3. After the detector had attained its desired temperature, injector heat was turned on and controlled

at 100°C.

4. The column heat was then turned on. Heat transfer from the detector and injector heat to column bath (thus raising column bath temperature even when the column heat setting is at zero) was observed. Therefore column bath temperature was controlled at 60°C with the dampers open to maintain a low temperature in the column.

5. The thermal conductivity cell power supply was switched on and the current through the filaments adjusted at 170 m Amperes to get optimum sensitivity without damaging the cell filaments.

6. The chart recorder was switched on after the equipment had stabilized.

7. The analysis of gases by the gas chromatograph and its calibration were carried out as detailed later.

The conditions of operation of the gas chromatograph are summarized in Table I.5 in Appendix I.

After the gas chromatograph components were stabilized, each of the gases expected to be encountered in the reactants and products was injected individually using the gas sampling valve.

Peak height obtained on the chart recorder for a pure gas sample introduced was considered to give a good quantitative estimate of the gas and a relationship was established between the quantity of a particular gas injected and the peak height. The residence time, which is defined

as the time elapsed between the moment the sample is introduced and when the maximum peak height is obtained, was also noted. This procedure was repeated for each of the gases.

The conditions of operation of the gas chromatograph were checked each day a run was made as these were found to vary slightly at times. The calibration of the chromatograph was also checked from day to day.

C. Operational Procedure

The reactor was charged with the required amount of catalyst mixed with the berl saddles. Berl saddles helped in the maintainance of uniformity in temperature of the catalyst bed. The thermocouple protection tubes were then held in place inside the catalyst bed 1 in. from each end of the bed. This was necessary to know the temperature distribution inside the catalyst bed.

Air from the compressed air line was allowed to pass through the system at the desired rate and the preheater furnace switched on for a few hours to allow the catalyst to attain constant activity. This was found necessary because the catalyst activity was found to deteriorate for the first few hours with air flowing in the system. The temperature of the preheater outlet gases was controlled by adjusting the power through the heating elements surrounding the preheater tube. The temperatures of the heating cords wound on the connecting tubing to control the heat losses of the gases in connecting tubing were also controlled

by separately controlled variable transformers.

The reactor feed gases were then fed to the system at the desired rate. The temperature at the top and the bottom of the reactor bed was regularly noted. Both of these temperatures were observed to rise continuously at a steady rate. However ~~a~~ the difference in temperature between the top and bottom part of the reactor was quite significant with the reactor top temperature 20 to 50°C above the reactor bottom temperature. If this were allowed to exist, the precision of the temperature at which the data is taken is completely lost.

To overcome this problem two methods were used in co-ordination with each other in order to be able to take the data at a particular temperature. In the first place, the temperature as indicated by the thermocouple in the top portion of the reactor was allowed to rise above the temperature level at which the data were desired. The reactor bottom temperature was also allowed to rise to a temperature level ~~which is~~ a few degrees below the desired temperature (the exact levels to which the top and bottom portion of the reactor should be allowed to rise can be decided only by experience). The heat input to the heating elements of the preheater and to the heating cords on the tube connecting the preheater to the reactor was then considerably reduced so that the temperature of the reactor top started falling after a while whereas reactor bottom temperature

continued to rise slowly till the temperature at which the data are taken ~~is~~ was reached simultaneously in both the reactor top and bottom portion. The product gases continued to pass through the gas sampling valve and were injected into the gas chromatograph at the proper instant. A minimum of two samples were analysed in this way for each run and the reproducibility of the results was carefully checked. The error in analysis by means of the gas chromatograph was ~~estimated~~ to be $\pm$ 3%.

VI. RESULTS AND DISCUSSION

The analysis of integral plug flow reactor data is much more difficult compared to either the differential reactor or the continuous stirred tank catalytic reactor. The use of the latter has very recently been demonstrated by Tajbl et. al. (24). Also the temperatures in the integral reactors are difficult to maintain especially for highly exothermic and highly endothermic reactions. The study of such reactions for significant conversions has, therefore, long been avoided under plug flow conditions.

Because of the design of the reactor and operating procedure developed during the course of this investigation, it was possible to study the kinetics of the highly exothermic catalytic oxidation of carbon monoxide in essentially a conventional integral plug flow reactor surrounded by an annulus through which the hot product gases pass and help in the maintenance of isothermal conditions in the reactor. This was achieved without any direct external heating of the reactor. The reactor bed temperatures could be controlled to a maximum variation of $\pm$ 2°C ($\pm$ 1°C for most of the runs) from the desired temperature. For an integral reactor, temperature control of this order can be considered as being very precise.

In order to avoid the effects of axial mixing upon the kinetics of the chemical reaction, the axial aspect ratio (Z/d_p) was considered carefully. An axial aspect ratio of 60 was used in this investigation in conformity with 30 or more suggested by Carberry (5,6). It was therefore ensured that axial mixing does not affect the reaction kinetics of carbon monoxide oxidation.

Radial heat transfer gradients were also considered to be important for this investigation. The passage of reactor outlet gases through the annulus surrounding the catalyst bed was found to be extremely helpful in controlling the radial heat transfer gradients at a low level. This was due to the fact that the gases flowing in the annulus were approximately at the same temperature as the reactor bed.

Mass and heat transfer effects were calculated and found to be negligibly small under the experimental conditions. The method of calculation is illustrated in Appendix IV.

Differentiation of the integral reactor data complicates the analysis and the data lose some precision. The equation of the plug flow catalytic reactor i.e.,

$$\frac{W}{F} = \int_0^{X_A} \frac{dX_A}{(-r_A)} \qquad \ldots(6.1)$$

can therefore be used in order to evaluate various models which will now be listed (26).

For the reaction,

$$aA + bB = rR$$

or,

$$\tfrac{1}{2}O_2 + CO = CO_2$$

the ~~mechanistic~~ rate equations for different rate controlling steps can be written as follows:

Controlling step	Rate Equation
Surface reaction between chemisorbed A and B	$k_s(a_A a_B - \frac{a_R}{K})\frac{K_A K_B}{(1+K_A a_A+K_B a_B+K_R a_R)^2}$ ...(6.2)
Adsorption of A without dissociation of A	$k_a(a_A - \frac{a_R}{K})\frac{1}{(1+\frac{K_A a_R}{K a_B} + K_B a_B+K_R a_R)}$ ...(6.3)
Adsorption of A with dissociation of A (all components other than A at equilibrium adsorption without dissociation)	$k_a(a_A - \frac{a_R}{K})\frac{1}{(1+\sqrt{\frac{K_A a_R}{K a_B}}+K_B a_B+K_R a_R)^2}$ ...(6.4)
Desorption of R	$k'_d(Ka_A a_B - a_R)\frac{1}{(1+K_A a_A+K_R a_R+KK_R a_A a_B)}$ ...(6.5)

The values for chemical equilibrium constant K for this reaction were calculated and found to be of the order of 10^{35}. The term a_R/K in all the above expressions can therefore be dropped. As mentioned in Chapter II, Stephens (22) has established that carbon monoxide is very highly

adsorbed on palladium surfaces. Assuming that the term $K_B a_B$ is very large as compared to the other adsorption terms. These simplifications lead one to the following equations:

For the case when surface reaction is rate controlling,

$$(-r_B) = k_s \frac{a_A a_B K_A K_B}{(1 + K_B a_B)^2} \qquad ...(6.6)$$

For high values of $K_B a_B$ ($K_B a_B \gg 1$), this reduces to the expression:

$$(-r_B) = k \frac{a_A}{a_B} \qquad ...(6.7)$$

With the adsorption of A without the dissociation of A as the rate controlling step, equation 6.3 is simplified to,

$$(-r_B) = k_a \frac{a_A}{(1+K_B a_B)} \qquad ...(6.8)$$

This equation for high values of $K_B a_B$ can be written as:

$$(-r_B) = k \frac{a_A}{a_B} \qquad ...(6.9)$$

which is the same as equation 6.7.

With dissociative adsorption of A as the rate controlling step, equation 6.4 can be written as:

$$(-r_B) = \frac{k\ a_A}{(1 + K_B a_B)^2} \qquad ...(6.10)$$

This equation for high adsorption of B reduces to,

$$(-r_B) = k \frac{a_A}{a_B^2} \qquad \ldots(6.11)$$

For desorption of R as the rate controlling step, the term Ka_Aa_B is very large compared to the term a_R in the numerator because of the very high value of K and therefore Eqn. 6.5 can be simplified to the following expression:

$$(-r_B) = k \qquad \ldots(6.12)$$

i.e., the rate of CO oxidation is independant of the concentration of the reactant and product species.

The right hand side of Eqn. 6.1 was then integrated using the simplified models listed above. The integrated expressions excluding the yet unknown multiplied term 1/k were plotted as absissae against W/F as ordinate. Equations 6.8, 6.10, and 6.11 gave non linear plots and were therefore rejected as plausible models,whereas Eqn. 6.12 was found to be inconsistent with the experimental data because the reaction rate was not found to be concentration independant and was rejected on this basis. A linear relationship is expected if the model being tested is correct. This criterion gives a sound method for the acceptance or rejection of a rate equation. Equations 6.7 and 6.9 which are essentially the same in their simplified forms gave straight lines on these plots at all the temperature levels (170^oC, 180^oC, and 195^oC) studied thus confirming the validity of the

model:

$$(-r_B) = k \frac{(O_2)}{(CO)} \qquad \ldots(6.7)$$

With this model, the integrated right hand side of eqn. 6.1 without the unknown factor 1/k can be written as:

$$\int \frac{(CO)}{(O_2)} dX_{CO} = \left[\left\{\ln\left(2\frac{(O_2)}{(CO)} - X_{CO}\right) - \ln\left(2\frac{(O_2)}{(CO)}\right)\right\} * \left(2\frac{(O_2)}{(CO)} - 1\right) + X_{CO}\right] * 2 \qquad \ldots(6.13)$$

The plots of the right hand side of eqn. 6.13 (without the unknown multiplied term 1/k) as abscissa against W/F as ordinate have been presented in Figs. 4, 5, and 6. These plots were then used to determine the slope which is equal to 1/k, from where k values at various temperatures were determined. All these plots gave straight lines passing through the origin within the limitations of the experimental errors. Obviously, this is one of the necessary conditions for the reaction rate model to be valid.

The k values determined from the slopes of these plots were then used to determine the energy of activation according to Arrhenius' law. Ln k was plotted as ordinate against 1/T as abscissa and a straight line relationship was obtained. The slope of this straight line gave the value of - E/R from where the energy of activation was computed. Statistical analysis showed that the model fitted the data within 95% confidence region. The energy

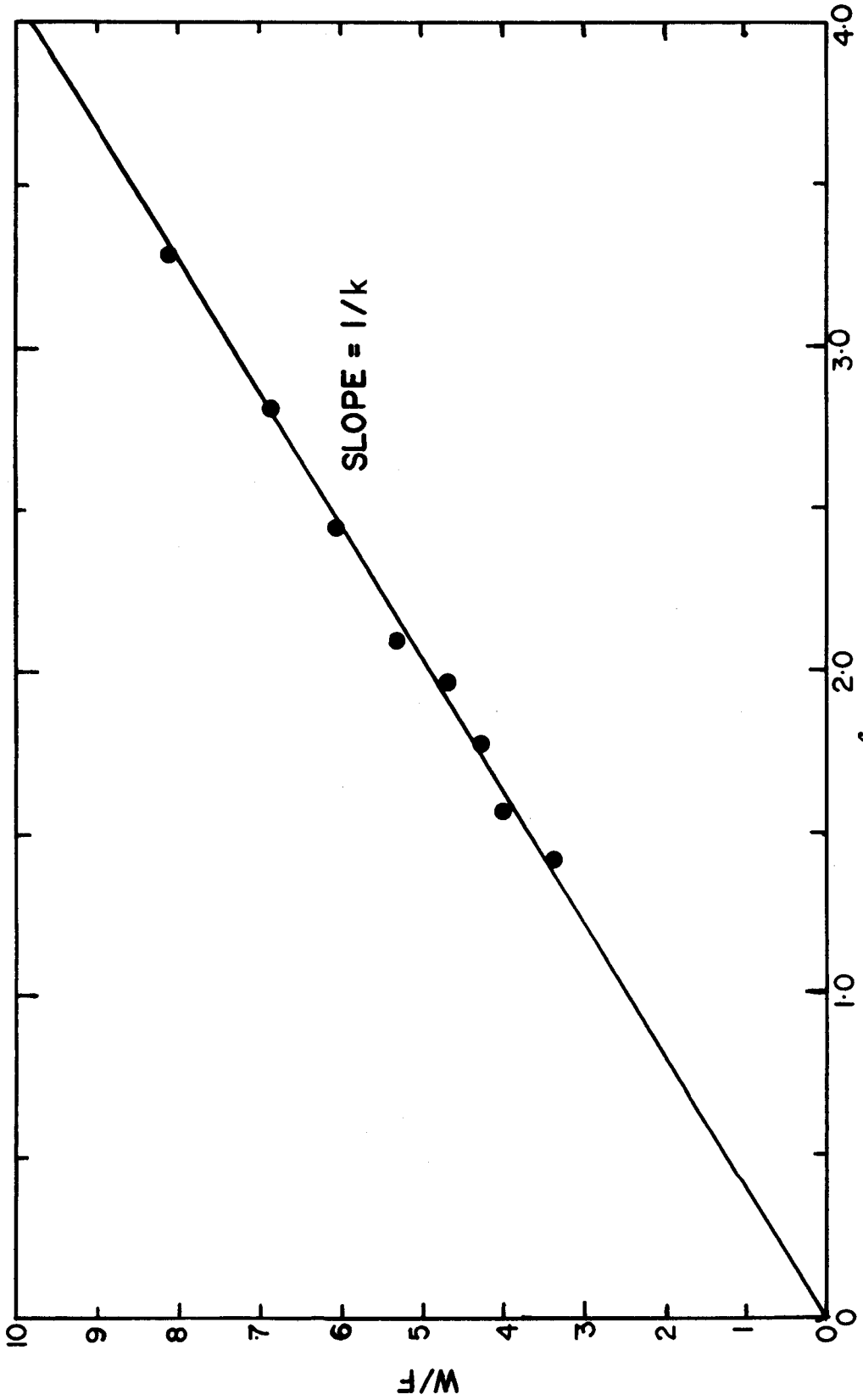

FIG. 4 MODEL FITTING TO DATA AT 170° C

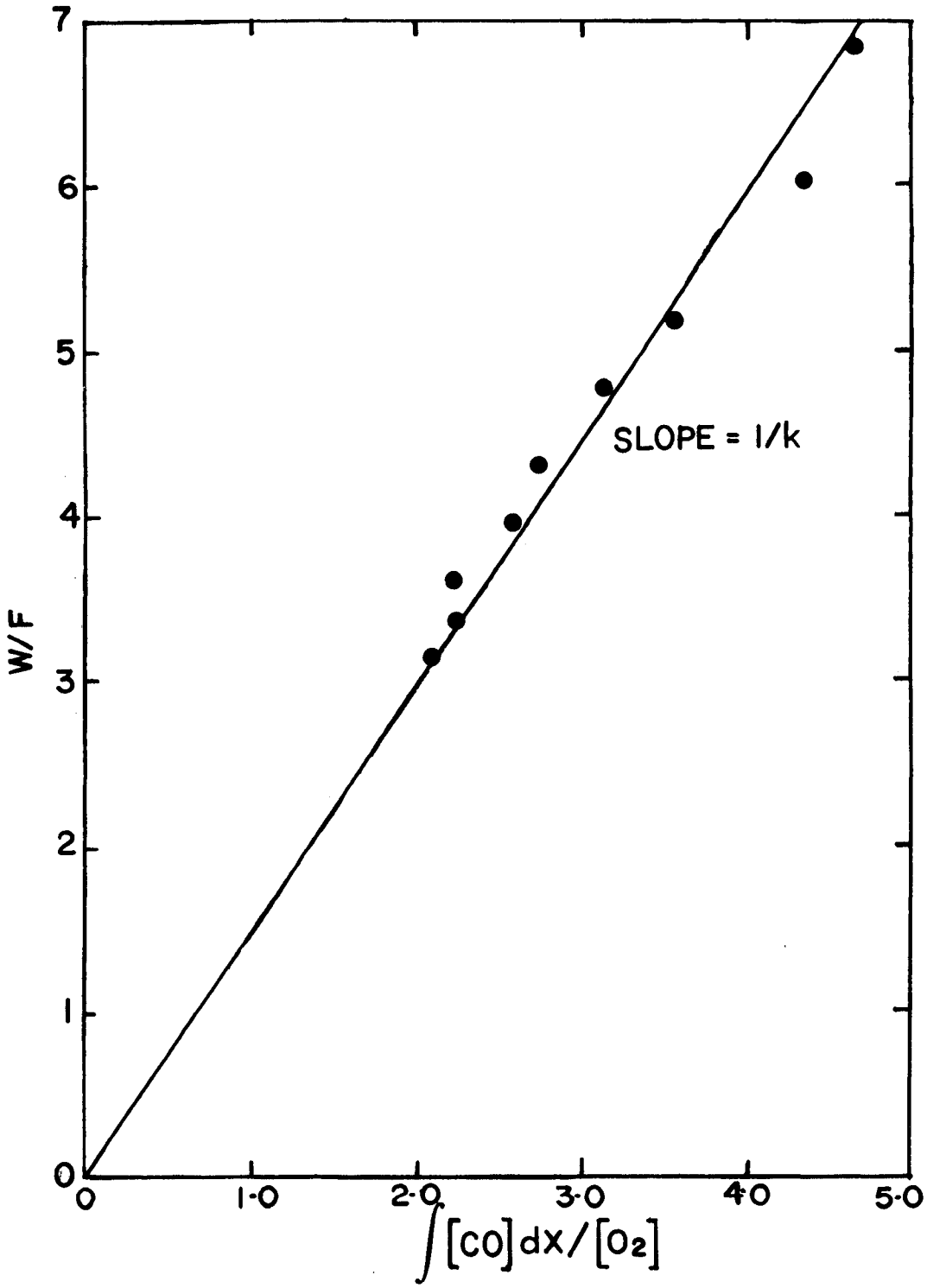

FIG.5 MODEL FITTING TO DATA AT 180°C

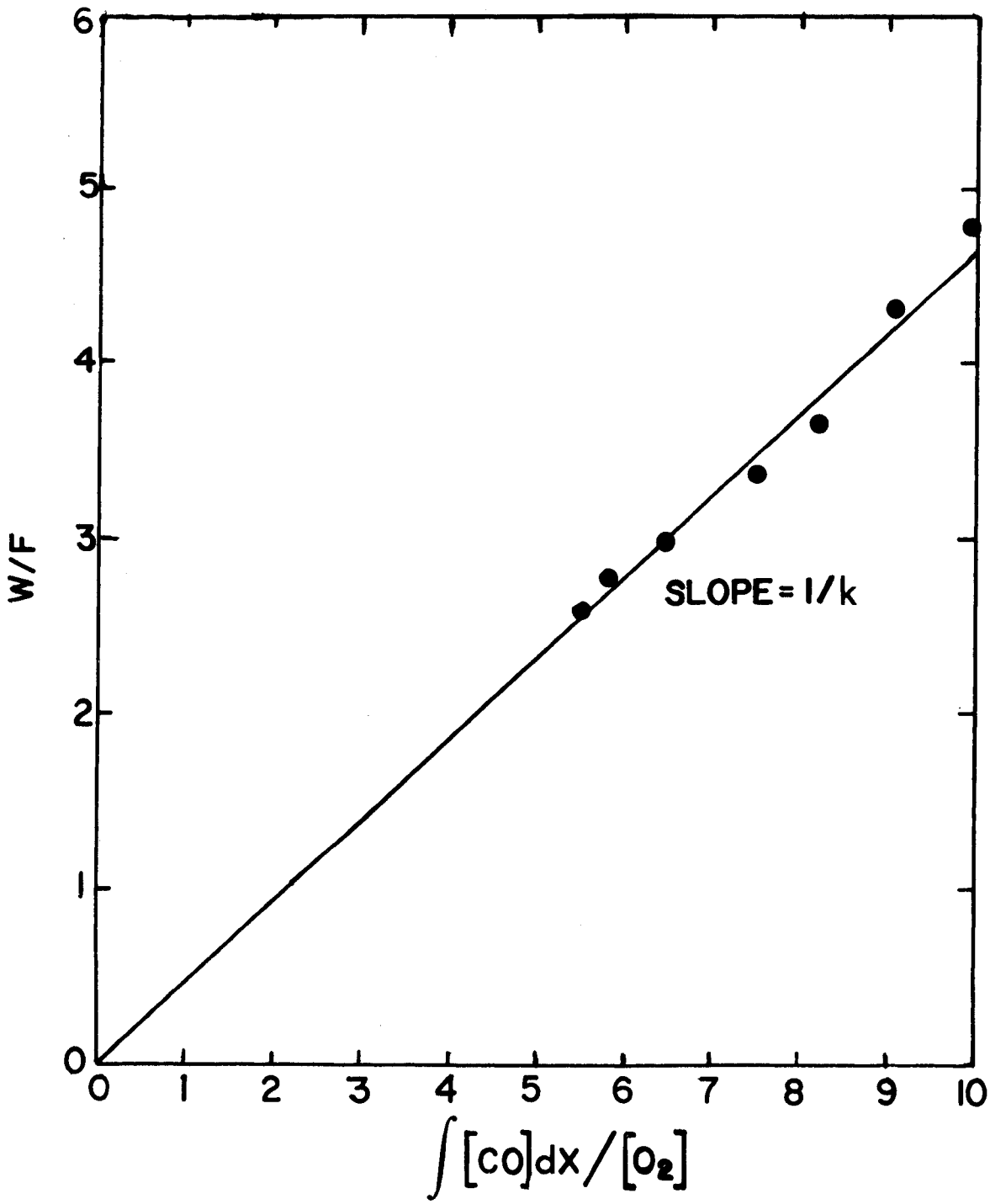

FIG.6 MODEL FITTING TO DATA AT 195°C

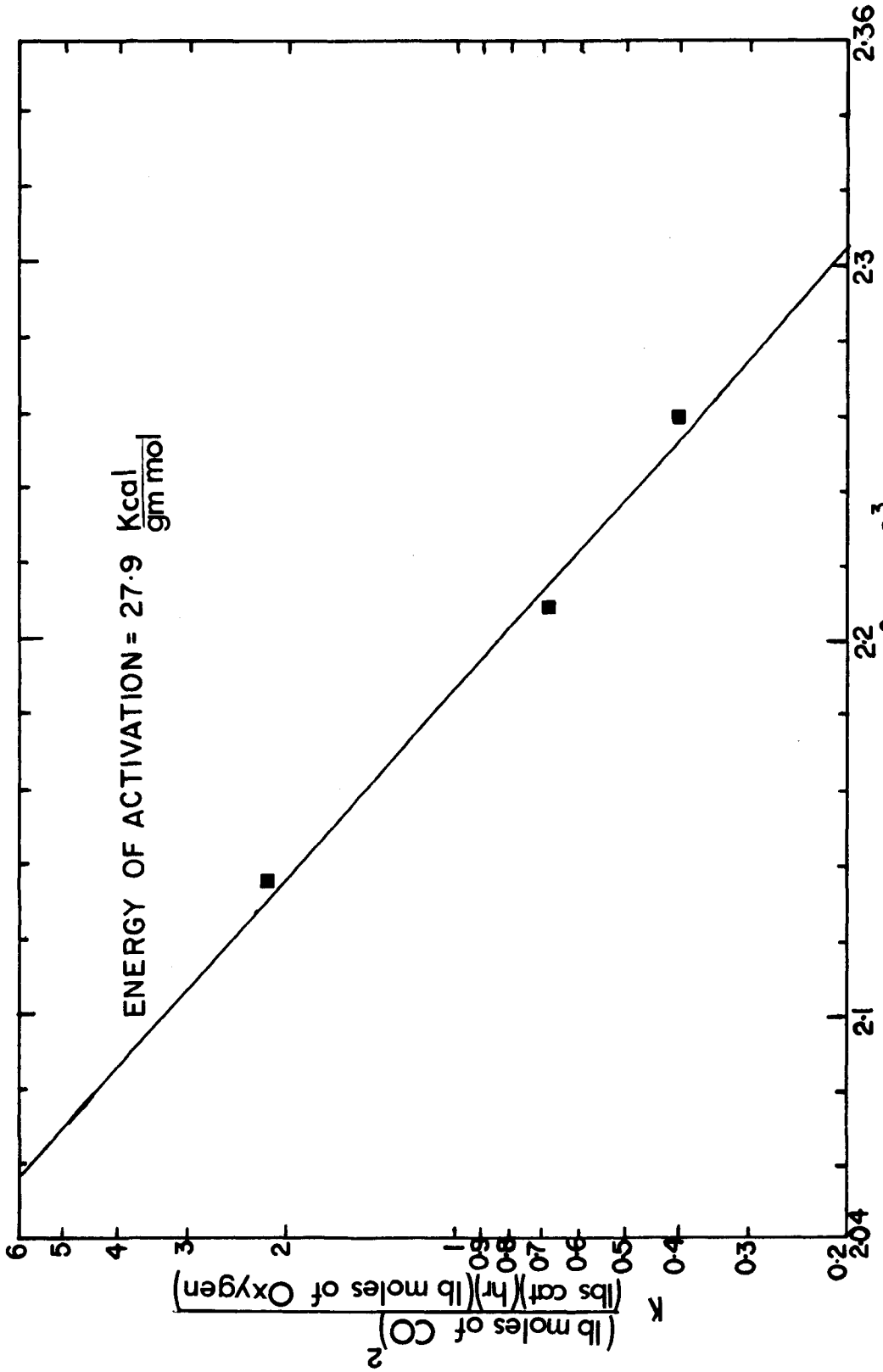

FIG.7 ARRHENIUS PLOT OF LOG K vs 1/T

of activation was found to be 27.9 ± 6.5 K.cals/gm. mole Table 6.1 lists a comparison of the results of this study with those of others.

TABLE 6.1

Comparison of Energies of Activation

Investigator	Catalyst	Temperature Range °C	E, Kcals. per gm. mole.
Schwab (21)	Pd wire	250-320	22.2 [a]
Daglish and Eley (7)	Pd wire	95-130	28.3 [b]
Modell (18)	Pd wire	140-150	28.7 [a]
Tajbl (24)	Pd on alumina	200-234	28.5 [a]
Present work	0.3 % Pd on alumina	170-195	27.9 [a]

[a] Based upon the rate model, $k(O_2)/(CO)$.

[b] Based upon the rate model, $k(O_2)/(CO)^2$.

The data on which the analysis of the present investigation is based are given in Tables III.1 to III.3 in Appendix III.

VII. CONCLUSIONS AND RECOMMENDATIONS

An experimental investigation has been carried out on the kinetics of the catalytic oxidation of carbon monoxide on 0.3 % Pd catalyst on alumina in an integral plug flow reactor with a modified design. The modified design and operating procedure kept the heat transfer gradients in the catalyst bed to a minimum. Isothermal conditions in the reactor could thus be achieved. This allowed precise control of temperature at the level at which the data were required. The axial aspect ratio, Z/d_p, was kept at a level that assured plug flow conditions.

The rate model for the system has been established and is found to conform to some of the earlier investigations (18, 21, 24) on Pd wire and on Pd on alumina catalyst, but disagrees with the investigation of Daglish and Eley (7).

The plots of $\int_0^{X_A} \frac{dX_A}{-r_A}$ against W/F allowed discrimination amongst rival rate models. The rate equation that described the data most satisfactorily is as follows:

$$-r_{CO} = 7.4\ e^{-27,900/RT}\ \frac{(O_2)}{(CO)}$$

where, $-r_{CO}$ = reaction rate in $\frac{\text{lb moles of CO converted}}{(\text{lb cat})\ (\text{hr})}$

R = gas constant, = 1.987 cals/(gm mole)(^oK)

T = temperature, ^oK

(O_2), (CO) = concentration of oxygen and carbon monoxide, respectively, (lb moles/cu ft);

which is a simplified form of the rate equation with either the oxygen chemisorption as the rate controlling step or the surface reaction between chemisorbed CO and O_2 as the rate controlling step. High adsorptivity of carbon monoxide on palladium has been established in the work of Stephens (22), and has been used in this investigation for the simplification of the control rate equations.

The validity of this rate model in conformity with the results of most of the other investigators indicates very strongly the possibility of use of the conventional plug flow reactors with the modified design in the study of highly exothermic catalytic reactions even at significant conversion levels.

It is therefore recommended that the feasibility of using such reactors with modified design be studied for other suitable reactions as well and that the integral plug flow catalytic reactor not be rejected premptorially.

NOMENCLATURE

A = component

a = concentration of reacting species, lb.moles/cu.ft.

a_m = area of particle per unit mass, $ft.^2/lb.$

a_v = area of particle per unit volume of bed, $ft.^2/ft.^3$

B = component

b = number of moles of B

C_p = heat capacity per unit mass at constant pressure

D = diffusion coefficient

D_{A-B}, D_{A-R} = diffusion coefficient in binary systems

D_{m-B} = diffusion coefficient (mean) of component B in a multicomponent system

E = Effectiveness factor

E = energy of activation

F = molal flow rate of CO, lb. moles/hr.

F = bulk mass flow rate of gases, lb. mass/hr.

G = mass velocity of gas based on total cross section of bed, $lbs./(ft.^2)(hr.)$

G_m = molal mass velocity of gas based on total cross section of the bed, $lb. moles/(ft.^2)(hr.)$

ΔH_B = molal heat of reaction of component B, Btu/lb. moles

j_D = mass transfer number

j_H = heat transfer number

K = adsorption equilibrium constant

k = reaction velocity constant

k = thermal conductivity

M = molecular weight

Pr = Prandtl number = $(Cp\mu)/k$

p_B = partial pressure of component B in ambient fluid, atm.

p_{Bi} = partial pressure of component B at the catalyst surface, atm.

p_{f_B} = pressure factor for component B

R = $r_{mB}/(a_m \phi G_m)$

Re = Reynolds number = $G/(a_v \phi \mu)$

r = number of moles of R

r_{mB} = molal reaction rate of component B, lb. moles of B converted/(hr.)(lb. of catalyst)

Sc = Schmidt number = $\mu/\rho D$

T = temperature, ^oK

t = time, hrs.

W = mass of the catalyst, lbs.

X = conversion, lb. moles of B converted/(lb. of catalyst)(hr.)

y_B = mole fraction of pressure factor

y_{fB} = mole fraction of pressure factor for component B

Greek Letters

Δ = difference

μ = viscosity of fluid, lb.mass/(ft.)(hr.)

π = total pressure, atm.

ρ = density of the fluid, lbs./ft.^{3}

ρ_s = bulk density of the catalyst bed, lbs of catalyst bed/ft.^{3}

Σ = summation

ϕ = shape factor

Subscripts

A,B,R = components

D = diffusion

f = film

H = heat transfer

i = component

m = mean

m = molal property

p = constant pressure

REFERENCES

1. Baker, M. McD. and G.I. Jenkins, Advances in Catalysis, Vol. VII, p. 1, Academic Press, Inc., New York (1955).

2. deBoer, J.H., Advances in Catalysis, Vol. VIII, p. 18, Academic Press Inc., New York (1956).

3. Caplan, John D., The Automobile Manufacturer's Vehicle Emissions Research Program, Jl. of Air Polln. Contr. Assn., 13 (3), 105 - 108 (1963).

4. Carberry, James J., First Order Rate Processes and Axial Dispersion in Packed Bed Reactors, Can. Jl. of Chem. Eng., 36, 207-209 (1958).

5. Carberry, James J., and M.M. Wendel, A Computer Model of the Fixed Bed Catalytic Reactors-The Adiabatic and Quasi-Adiabatic Cases, A.I.Ch.E. Jl., 9, (1), 129 (1963).

6. Carberry, James J., Designing Laboratory Catalytic Reactors, I.&E.C., 56, (11), 39-46 (1964)

7. Daglish, A.G. and D.D. Eley, The Carbon Monoxide-Oxygen Reaction on Palladium Gold Alloys, 2nd. International Congress on Catalysis, Vol. II, pp. 1615-1624 (1961).

8. DamKohler, G. and R. Edse, Z. Physik. Chem. B 53, 117 (1943)

9. Dixon, J.K. and J.E. Longfield, Catalysis, 7, 281 (1960).

10. Dixon, J.K. and J.E. Longfield, Catalysis, Vol. V, pp. 303-322, Reinhold Publishing Corporation, New York (1960).

11. Elliott, M.A., G.J. Nebel and F.G. Rounds, The Composition of Exhaust Gases from Diesel, Gasoline and Propane Powered Motor Coaches, Jl. of Air Polln. Contr. Assn., 5 (2), 103-108 (1955).

12. Faith, W.L., Automobile Exhaust Control Devices, Jl. of Air Polln. Contr. Assn., 13 (1), 33-35,39 (1963).

13. Hauffe, K., Advances in Catalysis, Vol. VII, p.213, Academic Press, Inc., New York (1955).

14. Hougen, O.A., Engineering Aspects of Solid Catalysts, I.&E.C., 53, (7), 509-528 (1961).

15. Hougen, O.A. and K.M. Watson, Chemical Process Principles, Vol. 3, John Wiley and Sons, Inc., New York (1947).

16. Katz, M., Advances in Catalysis, Vol. V, p. 177, Academic Press, Inc., New York (1953).

17. Lead in Gasoline Controvercy, Ch.E., 74, (3), 51 (1967).

18. Modell, M., D.Sc. Thesis, Massachusetts Institute of Technology, (1964).

19. Mulay, Avinash G., Catalytic Oxidation of Carbon Monoxide at Low Concentrations, Ph.D. Thesis, University of Wisconsin (1961).

20. Parravano, G. and M. Boudart, Advances in Catalysis, Vol. VII, p. 50, Academic Press, Inc., New York (1955).

21. Schwab, G.M., and K. Gossner, Z. Physik. Chem. Neue Folge, 16, 39 (1958).

22. Stephens S.J., Jl. Phys. Chem. 63, 188 (1959).

23. Suhrmann R., Advances in Catalysis, Vol. VII, p.303, Academic Press, Inc., New York (1955).

24. Tajbl, D.G., J.B. Simons, James J. Carberry, Heterogeneous Catalysis in a Continuous Stirred Tank Reactor, I.&E.C. Fundamentals 5, (2), 171-175 (1966).

25. Thomas, J.M., and W.J. Thomas, Introduction to the Principles of Heterogeneous Catalysis, p.453, Academic Press, London (1967).

26. Yang, K.H., and O.A. Hougen, Determination of Mechanism of Catalysed Gaseous Reactions, Chem. Eng. Prog. 46, (1), 146-157 (1950).

27. Yoshida, F., D. Ramaswami, and O.A. Hougen, Temperatures and Partial Pressures at the Surfaces of Catalyst particles, A.I.Ch.E. Journal, 8, (1), 5- (1962).

APPENDIX I

TABLES I.1 TO I.6

TABLE I.1 (11)

Constituents of Internal Combustion Engine
Exhaust Gases(Spark Ignition Engine)

Major Constituents (greater than 1 %)	Minor Constituents (lesser than 1 %)
Water	Oxides of sulphur
Carbon dioxide	Oxides of nitrogen
Nitrogen	Aldehydes
Oxygen	Organic acids
Carbon monoxide	Alcohols
Hydrogen	Hydrocarbons
	Smoke

TABLE I.2 (11)

Threshold Limits
For Continuous 8-Hour Exposure

Constituent	Parts per million by volume
Carbon dioxide	5,000
Carbon monoxide	100
Sulphur oxides	10
Formaldehyde	5
Nitrogen oxides	5

TABLE I.3 *

Effects of Carbon Monoxide Concentration on Human Body

Effects	CO concentration
Allowable for an exposure for eight hours	0.01 %
Can be inhaled for one hour without appreciable effect	0.04- 0.05 %
Causing a just appreciable effect after one hour of exposure	0.06- 0.07 %
Causing unpleasant symptoms, but not dangerous after one hour of exposure	0.1 - 0.12 %
Dangerous for exposure of one hour	0.15- 0.2 %
Fatal in exposure of less than one hour	0.4 and above

The commonly accepted value for the maximum allowable concentration for a daily 8-hour exposure is 100 ppm. This value has been accepted by the American Conference of Governmental Industrial Hygienists.

* Information supplied by the Matheson Company of Canada Ltd.

TABLE I.4*

Analysis of Commercial Grade Carbon Monoxide

Minimum purity	98.0 %
Carbon dioxide	2,000 ppm
Oxygen	20 ppm
Dew point	75 ppm

* Data supplied by the Matheson Company of Canada Ltd.

TABLE I.5

Operating Conditions of the Barber-Colman Selecta Series 5,000 Gas Chromatograph

Helium gas flow rate:	40 ml./mt.
Column temperature:	60°C
Injector temperature:	100°C
Detector temperature:	100°C
Detector filament current:	170 m.Amperes

TABLE I.6

Catalyst Details

The catalyst used for this investigation contained 0.3 % palladium activated and stabilized on high activity alumina supplied by the Harshaw Chemical Company. The physical properties of this catalyst were as follows:

Apparent bulk density:	55 lbs./cu. ft.
Surface area:	200 m^2 /gm.
Average side crushing strength:	22 lbs.
Pore volume:	0.40 c.c./gm.
Catalyst size	1/8" X 1/8" cylinderical pellets
Catalog no.	Pd.-0505 T

APPENDIX II

CALIBRATION CURVES

FIGURES 8 TO 14

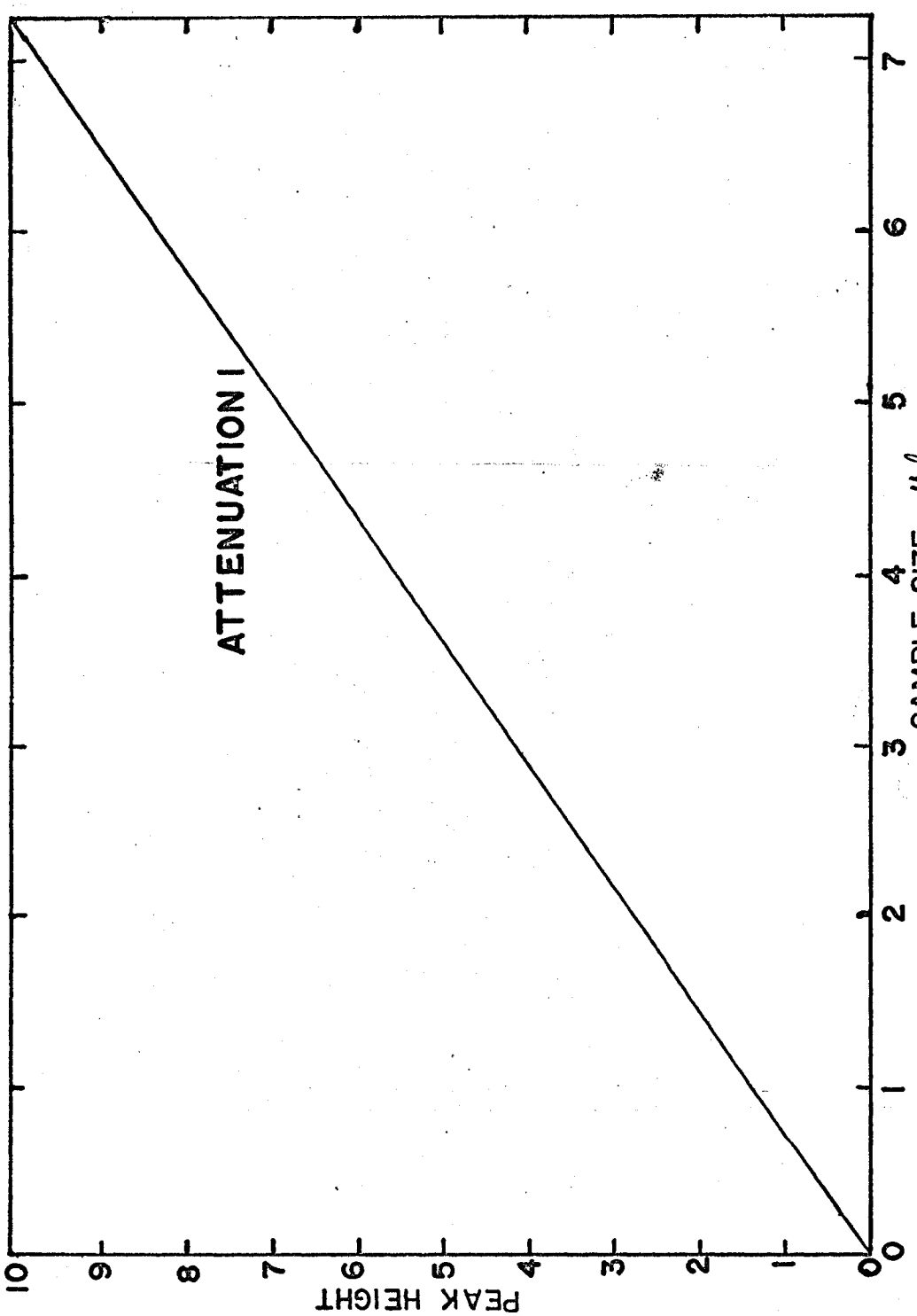

FIG. 8 G.C. CALIBRATION FOR OXYGEN GAS

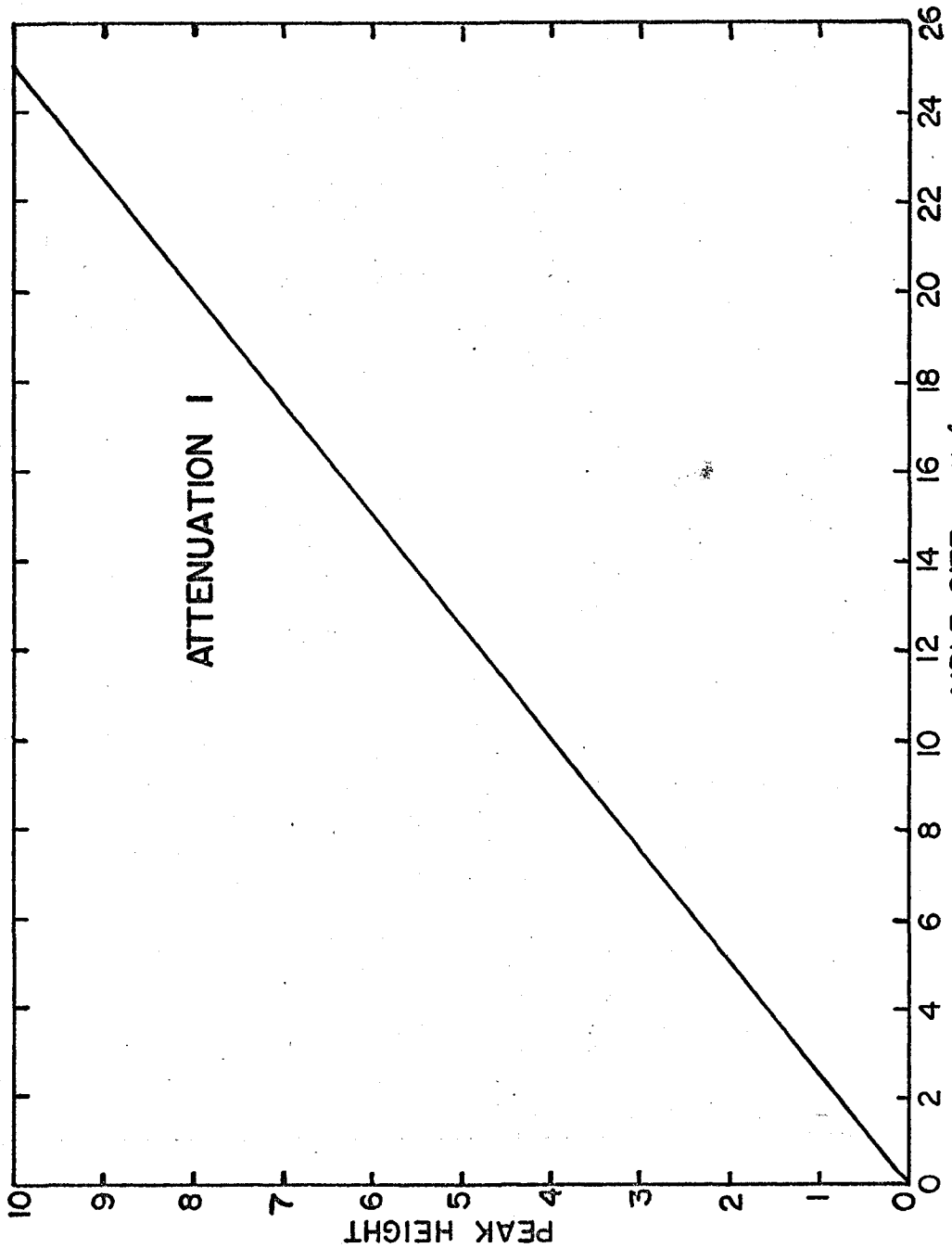

FIG. 9 G.C. CALIBRATION FOR CARBON MONOXIDE GAS

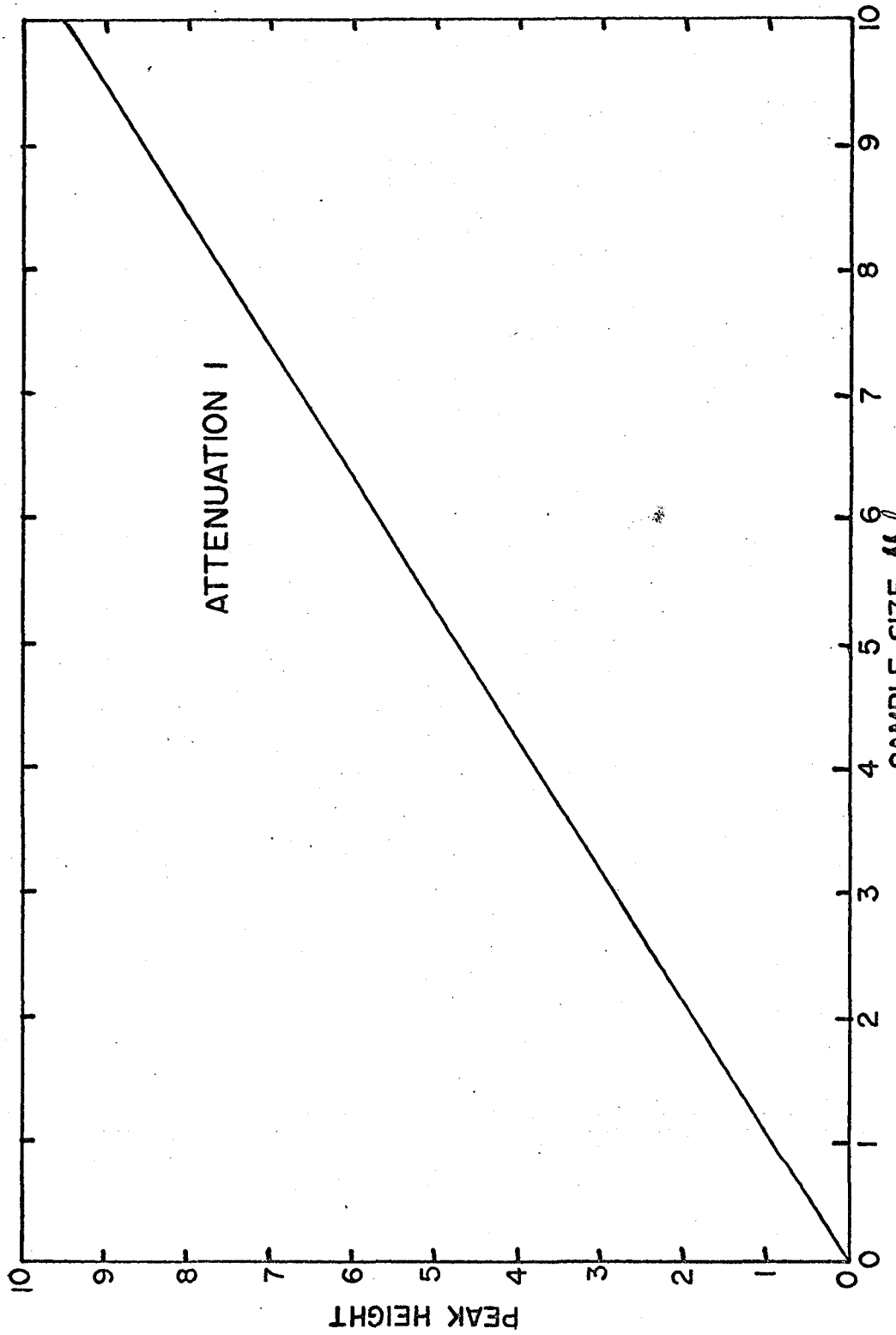

FIG. 10 G.C. CALIBRATION FOR CARBON DIOXIDE GAS

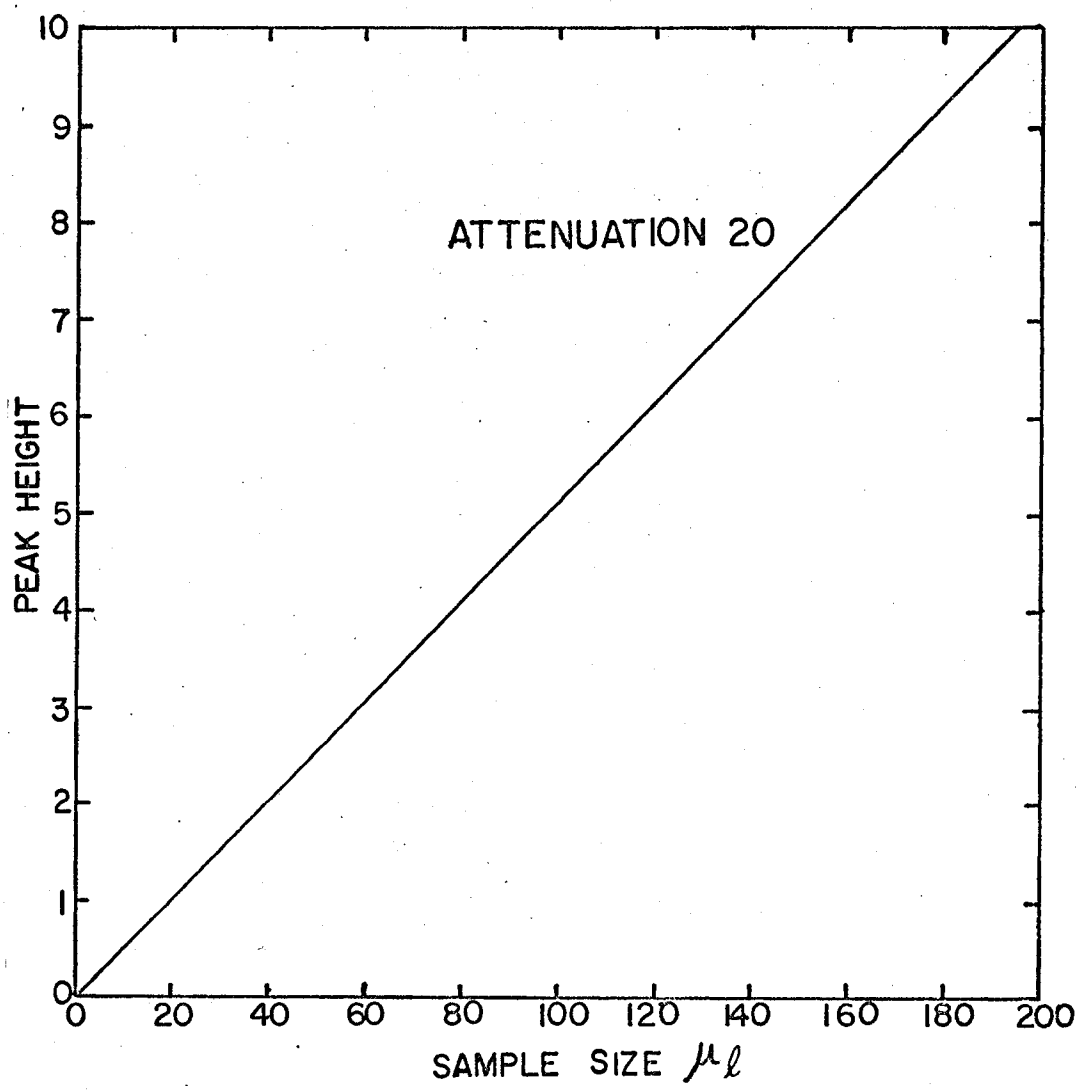

FIG. 11 G.C. CALIBRATION FOR NITROGEN GAS

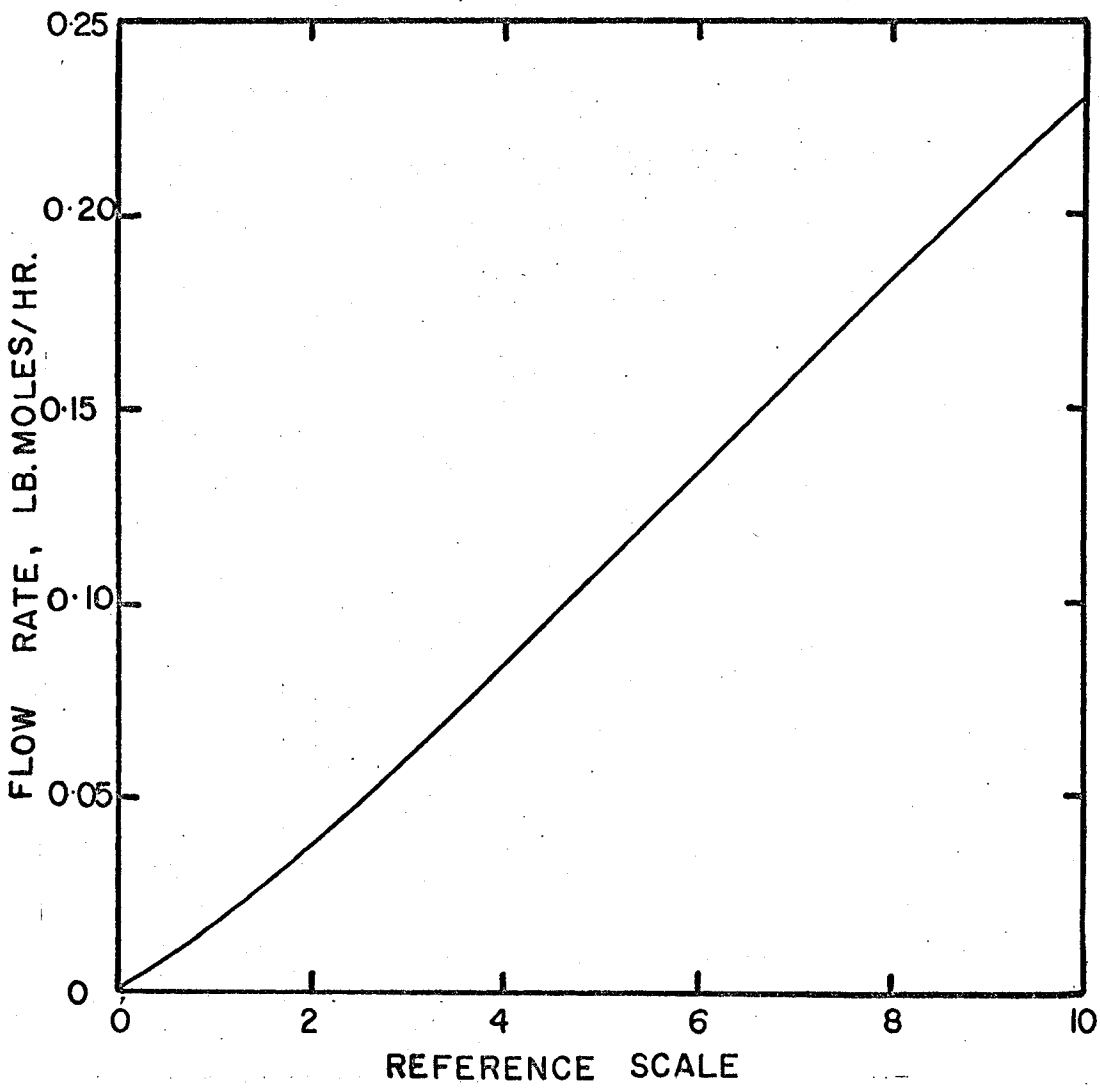

FIG. 12 CALIBRATION CURVE FOR AIR ROTAMETER AT 75°F

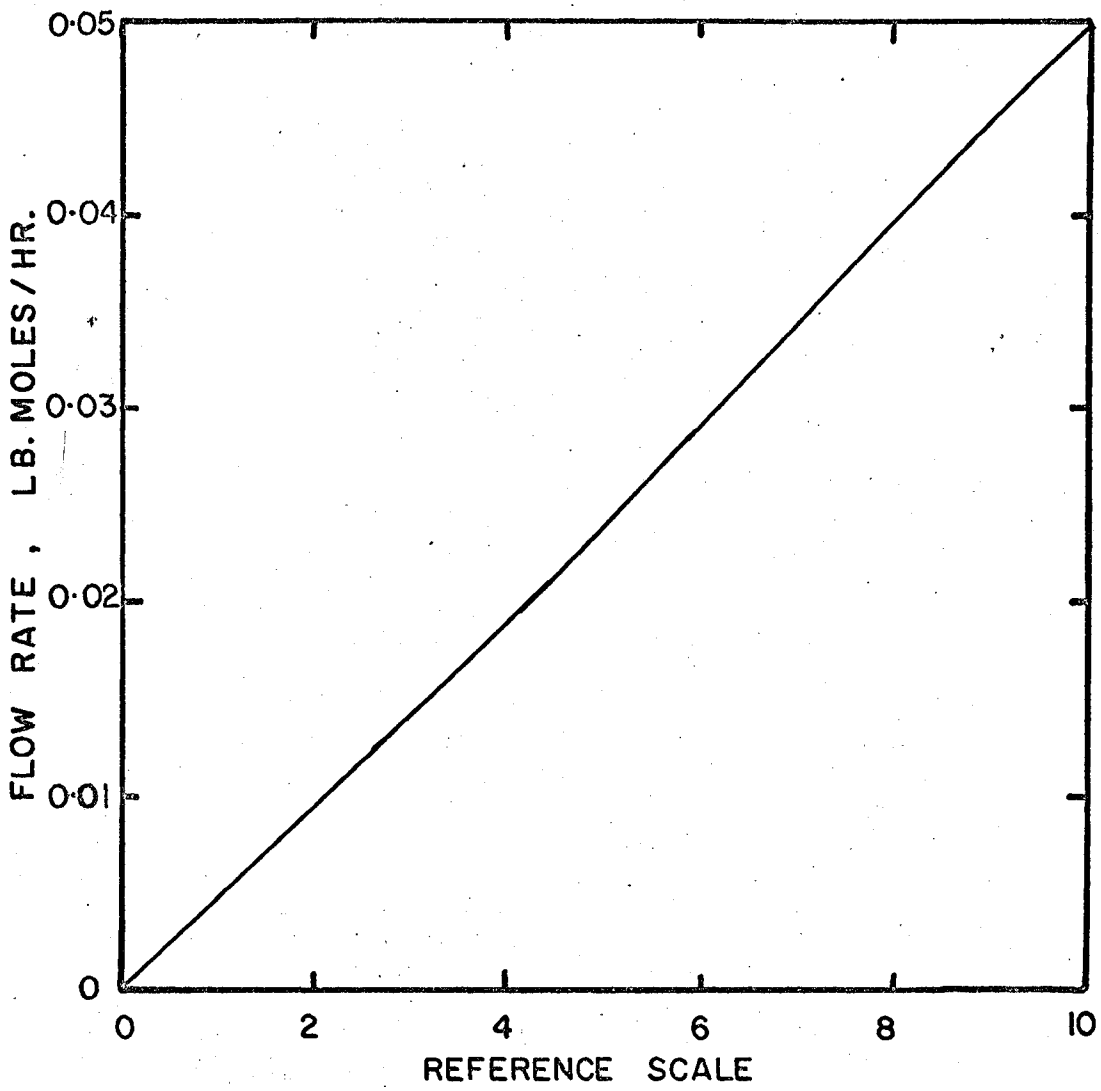

FIG.13 CALIBRATION CURVE FOR CARBON MONOXIDE ROTAMETER

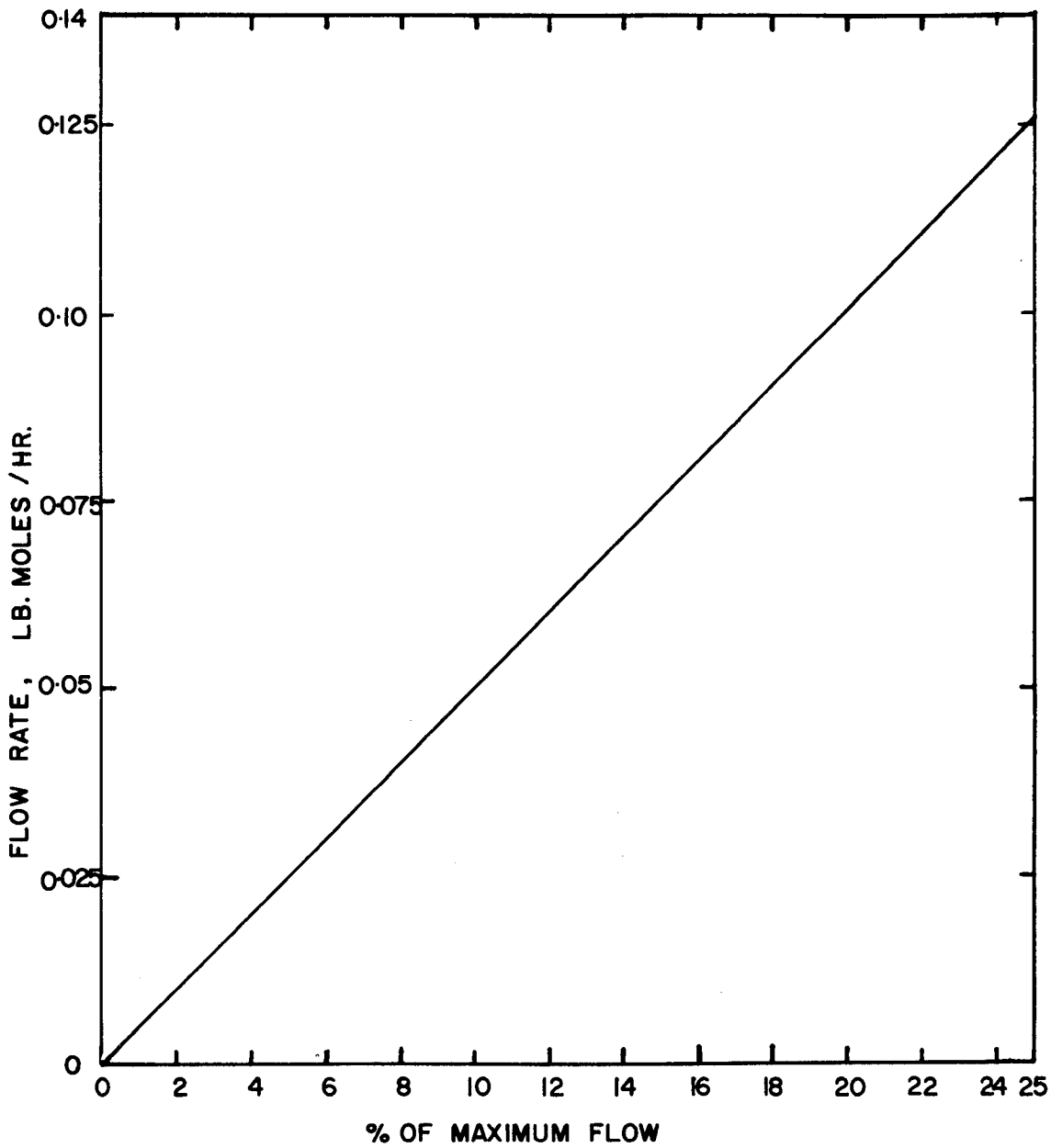

FIG. 14 CALIBRATION CURVE FOR NITROGEN ROTAMETER

APPENDIX III

EXPERIMENTAL DATA

Tables III.1 to III.3

TABLE III.1

TEMPERATURE	RUN NO.	W/F $\frac{\text{lbs. catalyst}}{\text{lb. moles of CO fed}}$	CONVERSION X_{CO} ± 4%	$\frac{(CO)}{(O_2)}\,dX$	k ± 7% from regression analysis
170°C	I.1	8.193	0.561	3.298	0.405
	I.2	6.929	0.607	2.821	
	I.3	6.014	0.587	2.406	
	I.4	5.314	0.565	2.102	
	I.5	4.773	0.520	1.978	
	I.6	4.325	0.502	1.737	
	I.7	3.941	0.473	1.585	
	I.8	3.359	0.412	1.427	

TABLE III.2

TEMPERATURE	RUN NO.	W/F $\frac{\text{lbs. catalyst}}{\text{lb. moles of CO fed}}$	CONVERSION X_{CO} ± 4%	$\frac{(CO)}{(C_2)}\,dX$	k ± 7% from regression analysis
	II.1	6.929	0.521	4.668	
	II.2	6.014	0.461	4.354	
	II.3	5.314	0.433	3.554	
	II.4	4.773	0.409	3.131	
180°C	II.5	4.325	0.391	2.766	0.673
	II.6	3.941	0.368	2.574	
	II.7	3.622	0.359	2.245	
	II.8	3.359	0.332	2.255	
	II.9	3.128	0.319	2.090	

TABLE III.3

TEMPERATURE	RUN NO.	W/F $\frac{\text{lbs. catalyst}}{\text{lb. moles of CO fed}}$	CONVERSION X_{CO} ± 4%	$\frac{(CO)}{(O_2)}\,dX$	k ± 7% from regression analysis
195°C	III.1	4.773	0.350	9.980	2.146
	III.2	4.325	0.316	9.113	
	III.3	3.622	0.264	8.211	
	III.4	3.359	0.243	7.459	
	III.5	2.964	0.222	6.444	
	III.6	2.771	0.210	5.810	
	III.7	2.608	0.199	5.525	

APPENDIX IV

MASS AND HEAT TRANSFER EFFECTS CALCULATIONS

APPENDIX IV

MASS AND HEAT TRANSFER EFFECTS

The mass and heat transfer effects at the surface of catalyst particles can be calculated using the method which has recently been presented by Yoshida et. al. (27). They have suggested correlations of the following types for evaluating these effects.

A. Mass Transfer Effects

The mass transfer effects can be computed from the knowledge of Reynolds numbers which can then be used to evaluate j_D values or used directly in Fig. 1 (27) along with the other parameter values as will be illustrated in this appendix. The theoretical correlations suggested are:

For $0.01 < Re < 50$,

$$j_D = 0.84\ Re^{-0.51} \qquad \ldots(IV.1)$$

For $50 < Re < 1{,}000$,

$$j_D = 0.57\ Re^{-0.41} \qquad \ldots(IV.2)$$

where Reynolds number is defined as

$$Re = \frac{G}{a_v \phi \mu} \qquad \ldots(IV.3)$$

and the equation which has been plotted as Fig. 1 by Yoshida et. al. is given as follows:

$$p_{CO} = R\,(j_D)^{-1}\,p_{f_{CO}}\,\left(\frac{\mu}{\rho D_{m-CO}}\right)^{2/3} \qquad \ldots(IV.4)$$

where R is $(r_m / a_m \phi G_m)$

For run number I.1,

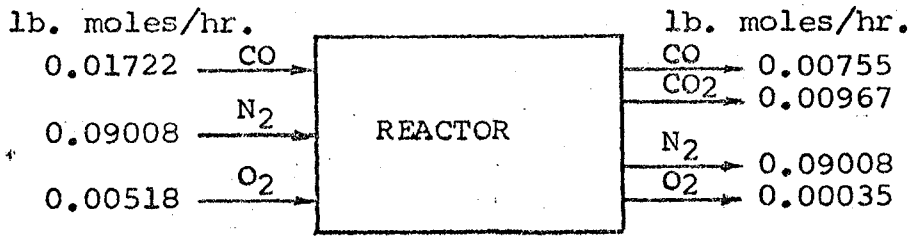

the rate of reaction is found to be

$$r_m = \frac{0.06}{0.65} = 0.0913 \frac{\text{lb. moles of CO converted}}{(\text{lbs. catalyst})(\text{hour})} \qquad \ldots(IV.5)$$

Mass of catalyst particles = 3.748 gms./100 particles

= 0.03748 gm./particle

Area of one catalyst particle(1/8"X 1/8"cylinder)

$$= \pi(1/8 \text{ X } 1/12)(1/8 \text{ X } 1/12) + 2 \text{ X } \frac{\pi}{4}(1/8 \text{ X } 1/12)^2$$

$$= 0.000511 \text{ ft.}^2/\text{particle}$$

then,

$$a_m = (0.000511/0.03748)(453.6) \text{ ft.}^2/\text{lb.}$$

$$= 6.16 \text{ ft.}^2/\text{lb.} \qquad \ldots(IV.6)$$

For cylinderical particles, $\phi = 0.91$

Also $$G_m = \frac{Fm}{A} = \frac{(0.11248 + 0.10765)/2}{(\pi/4)(1.37/12)^2}$$

$$= 10.75 \frac{\text{lb. moles}}{(\text{hr.})(\text{ft.})^2}$$

Therefore, $$R = \frac{r_m}{a_m \rho_{G_m}} = \frac{0.0815}{6.16 \times 0.91 \times 10.75} \quad \ldots(IV.7)$$

$$= 0.00135$$

and, $$a_v = a_m \rho_s \quad \ldots(IV.8)$$

$$= 6.16 \times 55 \ ft.^2/ft.^3$$

$$= 339 \ ft.^2/ft.^3$$

1. Partial Pressures

a. Inlet

$$P_{CO} = \frac{0.01722 \times \left(\frac{14.7 + 2.5}{14.7}\right)}{0.01722 + 0.0706 + 0.02463 + 0.79 + 0.02463 \times 0.21}$$

$$= \frac{0.01722 \times 17.2}{0.11248 \times 14.7} = 0.179 \text{ atm.}$$

$$P_{O_2} = \frac{0.02463 \times 0.21 \times 17.2}{0.11248 \times 14.7} = 0.053 \text{ atm.}$$

$$P_{N_2} = \frac{0.0706 + 0.02463 \times 0.79}{0.11248} \times \frac{17.2}{14.7}$$

$$= 0.938 \text{ atm.}$$

b. Outlet

$$P_{CO} = \frac{0.01722 \times 0.439}{0.10764} \times \frac{17.7}{14.7}$$

$$= 0.0845 \text{ atm.}$$

$$P_{O_2} = \frac{0.00035 \times 17.7}{0.10764 \times 14.7}$$

$$= 0.00392 \text{ atm.}$$

$$P_{CO_2} = \frac{0.00967 \times 17.7}{0.10764 \times 14.7} = 0.1083 \text{ atm.}$$

$$p_{N_2} = \frac{0.09008 \times 17.7}{0.10764 \times 14.7}$$

$$= 1.008 \text{ atm.}$$

c. Average Pressures

$p_{CO} = 0.1318$ atm.

$p_{O_2} = 0.02846$ atm.

$p_{CO_2} = 0.0541$ atm.

$p_{N_2} = 0.973$ atm.

2. Mean Physical Properties

a. Critical Temperature

$$T_{cm} = \sum_{i=1}^{n} X_i T_{ci}$$

$$= X_{CO} Tc_{CO} + X_{O_2} Tc_{O_2} + X_{CO_2} Tc_{CO_2} + X_{N_2} Tc_{N_2}$$

$$= 0.111 \times 133 + 0.024 \times 155 + 0.05015 \times 304 + 0.82 \times 126$$

$$= 137.97^{\circ}K$$

b. Average Molecular Weight

$$M_m = \sum_{i=1}^{n} X_i M_i$$

$$= 0.111 \times 28 + 0.024 \times 32 + 0.05015 \times 44 + 0.82 \times 28$$

$$= 29.05$$

c. Viscosity

Average viscosity of a gas mixture may be calculated from the critical viscosities of the individual gases in the mixture, the composition and reduced properties of the mixture. Using the correlations and figure given by Hougen and Watson (15), mean viscosity of the gas mixture is calculated as follows.

$$\mu_{cm} = \sum_{i=1}^{n} X_i \mu_{ci}$$

and $\mu_m = \mu_{cm} \times \mu_{rm}$

$$\mu_{cm} = (0.111 \times 190 + 0.024 \times 250 + 0.05015 \times 343 + 0.82 \times 180) \times 10^{-6} \text{ p.}$$

$$= 191.8 \times 10^{-6} \text{ p.}$$

Reading from Fig. 175, p. 871 (15) for,

$$T_r = \frac{170 + 273}{137.97} = 3.216$$

and $P_r = 0$

then, $\mu_{rm} = 1.2$

$$\mu_m = 191.8 \times 1.2 \times 10^{-6} \text{ p.}$$

$$= 230 \times 10^{-4} \text{ c.p.} = 230 \times 10^{-4} \times 2.42 \frac{\text{lbm.}}{(\text{ft.})(\text{hr.})}$$

$$= 0.0556 \frac{\text{lbm.}}{(\text{ft.})(\text{hr.})}$$

d. Density

The density of the gas mixture may be calculated from the average molecular weight.

$$\rho_m = \frac{29.05 \times (14.7 + 3.0) \times 273}{359 \times 14.7 \times (273 + 170)} \text{ lbs./cu. ft.}$$

$$= 0.0601 \text{ lbs./cu. ft.}$$

3. Diffusion Coefficients

The diffusion coefficients for diffusion between carbon monoxide and each of the rest of the gases can be computed using Eqn. 50 of reference (15), i.e.,

$$D_{A-B} = 0.0043 \frac{T^{3/2}}{\pi(v_A^{1/3} v_B^{1/3})^2} \sqrt{1/M_A + 1/M_B}$$

The values of atomic volumes (v's in the above expression) have been listed by Hougen and Watson in Table LIX (15).

The individual diffusion coefficients can now be computed.

$$D_{CO-O_2} = 0.0043 \frac{T^{3/2}}{\pi\left[(30.7)^{1/3}(25.6)^{1/3}\right]^2} \sqrt{1/28 + 1/32} \text{ cm.}^2/\text{hr.}$$

$$= 0.24 \text{ ft.}^2/\text{hr.}$$

$$D_{CO-CO_2} = 0.0043 \frac{T^{3/2}}{\pi\left[(30.7)^{1/3}(34.0)^{1/3}\right]^2} \sqrt{1/28 + 1/44} \text{ cm.}^2/\text{hr.}$$

$$= 0.1183 \text{ ft.}^2/\text{hr.}$$

$$D_{CO-N_2} = 0.0043 \frac{(443)^{3/2}}{\pi\,(30.7)^{1/3}(31.2)^{1/3}\,2}\sqrt{1/28 + 1/28} \quad cm.^2/hr.$$

$$= 0.358\ ft.^2/hr.$$

The diffusion coefficient of carbon monoxide with the rest of the gases may be calculated from the following correlation (15).

$$D_{CO-m} = \frac{1 - X_{CO}}{\frac{X_{O_2}}{D_{CO-O_2}} + \frac{X_{CO_2}}{D_{CO-CO_2}} + \frac{X_{N_2}}{D_{CO-N_2}}}$$

Using this, one gets,

$$D_{CO-m} = \frac{1 - 0.111}{\frac{0.024}{0.24} + \frac{0.05015}{0.1183} + \frac{0.82}{0.358}} \quad ft.^2/hr.$$

$$= 0.3108\ ft.^2/hr.$$

Mass velocity of the gas based on total cross section of bed is,

$$G = F/A = \frac{0.01722 \times 28 + 0.09008 \times 28 + 0.00518 \times 32}{(\pi/4)(1.37/12)^2}$$

$$= 311\ lbs./(hr.)(ft.^2)$$

Reynolds number as defined by Yoshida et. al.(27) may now be calculated.

$$Re = \frac{G}{a_v \phi \mu} = \frac{311}{339 \times 0.91 \times 0.0556}$$

$$= 18.13$$

Schmidt number is defined in the usual way,

$$Sc = \frac{\mu_m}{(\rho)(D_{CO-m})} = \frac{0.0556}{0.0601 \times 0.3108}$$

$$= 2.98$$

Also,

$$y_{f_{CO}} = 1 - y_{CO} \left(\frac{a + b - r}{b}\right) = 1 - y_{CO} \left(\frac{\frac{1}{2} + 1 - 1}{1}\right)$$

$$= 1 - 0.5\ y_{CO}$$

where $y_{CO} = \frac{p_{CO}}{\pi} = \frac{0.1318}{1.187} = 0.11$

then, $y_{f_{CO}} = 1 - 0.5 \times 0.11$

$$= 0.945$$

Using Fig 1 from (27), for a Reynolds number of 18.13, Schmidt number of 2.98, $y_{f_{CO}}$ of 0.945 and R value (Eqn.IV.7) of 0.001 , it is found that

$$y_{CO} = \frac{\Delta p_B}{\pi} = 0.013$$

therefore, $\Delta p_B = 0.013 \times 1.187$

$$= 0.01542 \text{ atm.}$$

which is a small fraction of the total pressure and is also

small compared to the partial pressure of carbon monoxide in the main gas stream, e.g., of all the runs at the temperature level of 170°C, the maximum partial pressure gradient between the main gas stream and the catalyst surface was found to be less than 8.5 % of the partial pressure of carbon monoxide in the main gas stream.

To consider the effect of this partial pressure gradient on the conversion of carbon monoxide, computation of inlet and outlet partial pressures at the catalyst interphase was made using a procedure which was essentially the same as that used earlier in this appendix. This however involved trial and error in which values of partial pressures at the interphase of the catalyst surface at the inlet and outlet were assumed and compared with those obtained by computation using Fig. 1 (27).

Based on the carbon monoxide partial pressures at the catalyst interphase at the reactor bed inlet and outlet conditions, partial pressure gradients were evaluated. These were then used to calculate the conversion of carbon monoxide thus taking mass transfer effects into account. This conversion was found to deviate less than 3.2 % from the conversion calculated without consideration of mass transfer effects. The effects were therefore considered negligible, and were neglected.

B. Heat Transfer Effects

The heat transfer gradients across the film surrounding the catalyst particles can also be calculated from the correlation given by Yoshida et. al. (27). The j_H factor may be obtained from the knowledge of j_D factor.

For $0.01 < Re < 50$,

$$j_D = 0.84(Re)^{-0.51}$$

then,

$$j_H = 1.076\ j_D$$

$$= 1.076 \times 0.84 \times (18.13)^{-0.51}$$

$$= 0.206$$

Average molal specific heats of the gases from 298°K to 443°K are as follows:

$$Cp_{mean\ CO} = 7.0 \text{ cals./(gm. mole)(°K)}$$

$$Cp_{mean\ O_2} = 7.2 \text{ cals./(gm. mole)(°K)}$$

$$Cp_{mean\ CO_2} = 9.65 \text{ cals./(gm. mole)(°K)}$$

$$Cp_{mean\ N_2} = 6.95 \text{ cals./(gm. mole)(°K)}$$

1. Specific Heat of the Mixture

$$Cp_{mix.} = \sum_{i=1}^{n} X_i\ C_{pi}$$

$$= 0.111 \times 7.0 + 0.024 \times 7.2$$

$$+ 0.05015 \times 9.65 + 0.82 \times 6.95$$

$$C_{pmix.} = 7.130 \frac{Btu}{(lb.\ moles)(^{\circ}R)}$$

$$= 7.130 \frac{Cals.}{(gm.\ moles)(^{\circ}K)}$$

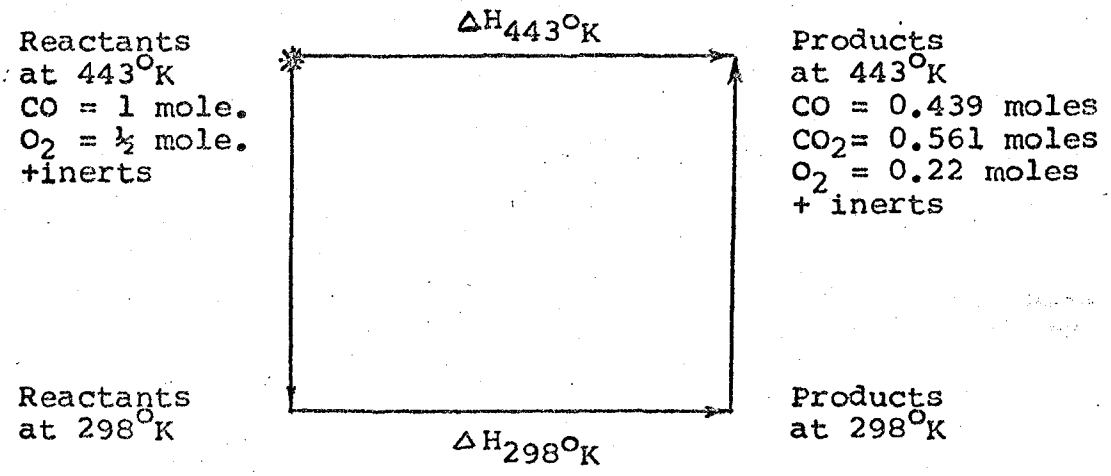

2. Heat of Cooling the reactants from 443°K to 298°K.

$$\Delta H_{cooling} = -(1 \times 7.0 + 0.5 \times 7.2)(443 - 298)$$

$$= -1.538 \text{ K. cals.}$$

3. Heat of Reaction at 298°K

$$CO \rightleftharpoons C + \tfrac{1}{2} O_2 \qquad \Delta H^{\circ}_{f298} = +26.416$$

$$C + O_2 \rightleftharpoons CO_2 \qquad \Delta H^{\circ}_{f298} = -94.052$$

$$(0.561)(CO + \tfrac{1}{2} O_2 \rightleftharpoons CO_2) \qquad \Delta H_{R298} = -67.636 \times 0.561$$

4. Heating the Products from 298°K to 443°K

$$\Delta H_{heating} = (0.439 \times 7.0 + 0.561 \times 9.65 + (0.5 - 0.561/2) \times 7.2) \times (443 - 298)$$

$\Delta H_{heating}$ = 1.460 K. cals.

Heat of reaction at 443°K may now be computed from the information gained above.

$$\Delta H_{R\ 443^{\circ}K} = -1.538 - 67.636 + 1.460$$

$$= -67.714 \text{ K. cals./gm. mole of CO fed}$$

$$= -\frac{67.714 \times 10^{3}}{1.8} \text{ Btu/lb. mole of CO fed}$$

$$= -37{,}600 \text{ Btu/lb. mole of CO fed}$$

5. Prandtl Number

Using the relationship given by Eqn. 51 (15)

$$Pr = \frac{4}{9 - 5C_v/C_p} = \frac{4}{9 - 5 \times \frac{5.15}{7.13}}$$

$$= 0.743$$

Then the temperature differential across the film separating the main gas stream and the catalyst surface can be calculated from the following expression given by Yoshida et. al. (27).

$$\frac{\Delta t}{T} = \frac{r_{m-co}\ \Delta H_{R\ co}}{a_m \phi\ Cp\ G_m\ T} (j_H)^{-1}(Pr)^{2/3}$$

Subsituting the values of the various terms occuring in this from those calculated earlier,

$$\Delta t/T = \frac{0.0815 \times 37{,}600 \times (0.206)^{-1}}{6.16 \times 0.91 \times 7.130 \times 10.98 \times 766}(0.743)^{2/3}$$

or, $$\frac{\Delta t}{T} = 0.0348$$

i.e., $$\% \frac{\Delta t}{T} = 3.48\ \%$$

which is very small in magnitude for the conditions at which this investigation has been carried out, and can therefore be safely neglected without any significant effects on the results.

VITA AUCTORIS

1945 Born in Moga, Panjab, India.

1966 Received the Bachelor of Science degree in Chemical Engineering from the Department of Chemical Engineering and Technology, Panjab University, Chandigarh, India.

1966 Accepted into the Graduate School of the University of Windsor, Windsor, Ontario as a candidate for the degree of Master of Applied Science in Chemical Engineering.